First posted online on 28 May 2020 as 10.1242/dev.188987
Access the most recent version at http://dev.biologists.org/lookup/doi/10.1242/dev.188987

The stem-like STAT3-responsive cells of zebrafish intestine are WNT/β-catenin dependent.

Margherita Peron*, Alberto Dinarello*, Giacomo Meneghetti, Laura Martorano, Nicola Facchinello, Andrea Vettori, Giorgio Licciardello, Natascia Tiso, Francesco Argenton.

Dipartimento di Biologia, Università degli Studi di Padova, Via Ugo Bassi 58b, Padova, ITALY.
*These authors contributed equally to this work.

KEYWORDS: Stat3, Stem cells, Intestine, Zebrafish, Wnt/β-catenin

ABSTRACT

The transcription factor STAT3 is required for proliferation and pluripotency of embryonic stem cells; we have prepared and characterized fluorescent STAT3-reporter zebrafish based on repeats of minimal responsive elements. These transgenic lines mimic *in vivo* STAT3 expression patterns and are responsive to exogenous STAT3; notably, fluorescence is inhibited by both *stat3* knock-out and IL6/JAK/STAT inhibitors. At larval stages, STAT3 reporter activity correlates with proliferating regions of the brain, haematopoietic tissue and intestine. In the adult gut the reporter is active in sparse proliferating cells, located at the base of intestinal folds, expressing the stemness marker *sox9b* and having the mammalian Crypt Base Columnar cells morphology; noteworthy, zebrafish *stat3* mutants show defects in intestinal folding. The STAT3 reporter activity in the gut is abolished in mutants of Tcf7l2, the intestinal mediator of Wnt/β-catenin-dependent transcription, and the Wnt/β-catenin dependence of STAT3 activity in the gut is confirmed by abrupt expansion of STAT3-positive cells in intestinal adenomas of *apc* heterozygotes. Our findings indicate that Jak/STAT3 signalling is needed for intestinal stem cells maintenance and possibly crucial in controlling Wnt/β-catenin-dependent colorectal cancer cells proliferation.

INTRODUCTION

Signal Transducer and Activator of Transcription 3 (STAT3), the most prominent member of the STAT family of proteins, is involved in a plethora of cellular processes including development, differentiation, inflammation and metabolism (Levy and Lee; 2002). In mammals STAT3 is typically activated by Janus Kinase (JAK) 2-mediated phosphorylation of its tyrosine at position 705. Once phosphorylated at Y705, STAT3 dimerizes, translocates in the nucleus and binds to responsive elements (SRE) in the regulatory regions of its target genes.

One of the most remarkable functions of STAT3 is its role in preserving the full differentiative potential of stem cells in several tissues. Indeed, STAT3 is required for self-renewal of mouse embryonic stem cells (Raz *et al.*, 1999), survival of murine small-intestine crypts (Matthews *et al.,* 2011), maintenance of neural precursors as well as for regulation of haematopoiesis and muscle regeneration of adult mice (Galoczova *et al.,* 2018). While STAT3 phosphorylation is strictly regulated in physiological conditions, over-activation of STAT3 has been detected in a variety of human cancers, suggesting a key role for this transcription factor in tumour initiation and progression (Huynh *et al.,* 2019). In haematopoietic malignancies and solid tumours, the chronic inflammatory conditions and the maintenance of cancer stem cell properties were reported to be dependent on IL-6/STAT3 axis, which also stimulates the self-renewal of neoplastic cells (Pattabiraman *et al.,* 2014; Johnson et *al.,* 2018). In particular, the importance of JAK/STAT3 signalling in intestinal tumorigenesis is well-established and associated with the hyper-proliferative and invasive phenotype of human colorectal cancer (CRC) (Wang *et al.,* 2014). While IL-6/STAT3 signalling alters mucosal barrier in colon adenomas, accelerating the adenocarcinomas transition, it is also well-known that Wnt/β-catenin pathway plays an essential role in gut homeostasis (Ahmad *et al.,* 2017). In fact, it has been reported that the hyper-activated Wnt/β-catenin signalling induces epithelial to mesenchymal transition and promotes CRC (Morin *et al.,* 1997; Vu and Datta, 2017), indicating that the two signalling pathways are both acting in CRC pathogenesis and progression (Ahmad *et al.,* 2017).

Germline transformed zebrafish embryos expressing fluorescent protein-coding genes under the control of specific promoters and enhancers allow to follow gene regulation in specific cell populations at single-cell resolution. These transgenic animals, either

embryos, larvae or adults, can be studied with digital time lapse, image quantification, FACS sorting and mass sequencing at specific times and in specific tissues. In addition, global fluorescence can be used as an output for screening new compounds as well as for drugs repurposing (Gallardo *et al*., 2013). This approach is largely used to study entire promoters but, lately, has been improved by utilising multimerized elements purely responding to single transcription factors (Moro *et al.,* 2013). *In vitro* studies have shown that the TTCCCGAA sequence taken from the C-reactive protein (CRP) promoter (CRP acute phase response element CRP-APRE) is able to selectively mediate STAT3 transcriptional activities in response to IL-6 in Hep3B cells (Zhang *et al.,* 1996). As a consequence, multimerized CRP-APRE has been largely used as a *bona-fide* STAT3 specific reporter in mammalian cells (Turkson *et al.,* 1998). Taking advantage of zebrafish reporter lines as living biosensor and the knowledge on the specificity of CRP-APRE as STAT3 responsive elements, we generated a STAT3 transgenic reporter to clarify *in vivo* the role of this transcription factor during embryonic and larval development, in adults and in intestinal cancer models. Our analyses reveal that STAT3 activity is tightly linked with proliferation, that STAT3-responsive cells of zebrafish intestinal folds colocalize with the stemness marker Sox9b (Aghaallaei *et al.,* 2016), and that gut cellular activities are dependent on a WNT/β-catenin/STAT3 signalling cascade, both during tissue formation and tumour growth.

RESULTS

The zebrafish *Tg(7xStat3-Hsv.Ul23:EGFP)* fluorescent line reveals regions of Stat3 transcriptional activity.

With the aim of detecting Stat3 responsive cells in the developing zebrafish embryos, we generated a zebrafish transgenic line in which tandemly repeated Stat3 responsive elements are used to drive a fluorescent reporter (Moro *et al.,* 2012; Moro *et al.,* 2013). To this purpose, seven repeats containing the Stat3 responsive element (TTCCCGAA) from the human C-reactive protein gene promoter were taken from pLucTKS3 construct (Turkson et al., 1998), cloned upstream of a 24-bp fragment of the herpes simplex virus thymidine kinase (Hsv.Ul23) promoter and used to create the Tol2 Gateway destination vector pDest(7xStat3-Hsv.Ul23:EGFP) (Fig. 1 A)(Kwan *et al.,* 2007). One-cell stage embryos injected with the destination vector were raised to adulthood and outcrossed

with WT fish in order to isolate founders carrying the transgenic cassette in the germ-line. F1 progenies from single founders, selected based on their Mendelian transmission and reporter signal intensity, were raised to adulthood to establish the stable and hemizygous transgenic line *Tg(7xStat3-Hsv.Ul23:EGFP)* (from now on called Tg(*7XStat3:EGFP)*).

The reporter expression is already detectable shortly after fertilization: when eggs are laid by a *Tg(7xStat3:EGFP)* female, embryos display ubiquitous EGFP expression already at 1-cell stage. On the other hand, no EGFP is detectable in 1-cell stage embryos obtained by outcrossing *Tg(7xStat3:EGFP)* males with WT females, thus indicating that the reporter is maternally activated in the oocyte during oogenesis (Fig. 1 B, B'). High levels of zygotic transgene expression start to be detected during late somitogenesis (22 hpf, hours post fertilization) in the anterior telencephalon (Fig. 1 C), in the primordium of the Midbrain Hindbrain Boundary (MHB) and in cells of the hindbrain region that possibly define the precursors of zebrafish cranial ganglia (Fig. 1 D). In addition, at the same stage of development, *Tg(7xStat3:EGFP)* transgene expression can be detected in neuromast precursor cells of the head and lateral line (Fig. 1 E). Finally, the developing haematopoietic tissue, that in zebrafish is topologically identified, posteriorly to the yolk extension in the intermediate cell mass (ICM), reveals a strong transgene activity detectable from 19-20 hpf (Fig. 1 F), consistent with the known activity of Stat3 during mammalian hematopoietic stem cell regeneration (Chung., 2006). This was also confirmed by crossing the *Tg(7xStat3:EGFP)* line with the *Tg(gata1a:DsRed)*^{sd2} line that labels erythroid progenitor cells (Traver *et al.,* 2003) and observing at 22 hpf that the two fluorescent proteins are partially co-expressed in cells of the haematopoietic tissue (Fig. S1). At 48 hpf, *Tg(7xStat3:EGFP)* activity is mostly located in cells of the Optic Tectum (TeO), a tissue known to be rapidly proliferating and differentiating at this stage (Fig. 1 G, H) (Recher *et al*., 2013). EGFP expression in TeO is inversely proportional to the differentiation gradient, being stronger in the Peripheral Midbrain Layer (PML) of the TeO and then progressively fading at the centre of the lobe (Fig. 1 H). More detailed information concerning Stat3 reporter expression in the CNS was obtained by VIBE-Z imaging (Ronneberger *et al.,* 2012) of 3-days post fertilization (dpf) larvae. At this stage, *Tg(7xStat3:EGFP)* activity was also found in the forebrain (*subpallium*, preoptic region and hypothalamus) and the retinal layer (Fig. S2, Movie 1). Starting from 4 dpf, a strong EGFP expression is detected in a restricted population of pear-shaped cells of the

developing intestine (Fig. 1 I); notably, this "salt and pepper" EGFP fluorescence is maintained in the adult intestine (Fig. 1 J).

Noteworthy, Stat3 reporter fluorescence reflects *stat3* mRNA expression domains at all stages of zebrafish embryonic development, including telencephalon, retina, cranial ganglia, lateral line system and TeO, as already described by Thisse *et al.* (2004). In order to further assess Stat3 reporter responsiveness, we provided the embryos with two known chemical inhibitors of the pathway: AG-490, a known Jak2 kinase inhibitor, and LLL12, a molecular competitor that binds specifically to the dimerization binding region of the Stat3 protein, thus preventing its nuclear translocation (Lin *et al.,* 2010)(Meydan *et al.,* 1996). Both AG-490 and LLL12 treatments resulted in a significant reduction of EGFP expression in the TeO compared to control (Fig. 2 A, A'); moreover, AG-490 treatment between 3 and 6 dpf abolished almost completely EGFP intestinal expression in *Tg(7xStat3:EGFP)* larvae (Fig. 2 B, B').

To test their positive responsiveness to STAT3, we injected 1-cell stage *Tg(7xStat3:EGFP)* embryos with an mRNA encoding a constitutively active form of murine STAT3 harbouring cysteine substitutions at the 661 and 663 residues (m*Stat3C*). These modifications force the formation of disulphide bridges and the consequential induction of a constitutively active STAT3 dimer (Sellier *et al.*, 2013). Embryos injected with m*Stat3C* mRNA displayed an ectopic and significant increase of EGFP fluorescence (Fig. S3 A, A'), hence confirming that *Tg(7xStat3:EGFP)* reporter responsiveness *in vivo* is, *bona-fide*, STAT3 dependent. These data are also confirmed by the immunofluorescence performed in *Tg(7xStat3:EGFP)* larvae injected with CMV-m*Stat3C* plasmid and showing mosaic co-localization of EGFP ectopic signal and mouse STAT3 protein (Fig. 2D). In addition, we have generated the CRISPR/Cas9 *stat3*$^{ia23/ia23}$ KO line, from now on named *stat3*$^{-/-}$. *stat3*$^{-/-}$ fish are predicted to encode a truncated protein of 456 amino acids, thus lacking all functional domains including the DNA-binding domain, the dimerization domain and the transactivation domain (Fig. S4 A). At 6 dpf, *stat3* mutant larvae show both a significant reduction of mutant RNA expression (Fig. S4 B), consistent with nonsense RNA decay thus confirming the null nature of this allele, and a significant decrease in the transcription of two known Stat3 target genes such as *socs3a* and *cebpb,* (Fig. S4 C). Notably, *Tg(7xStat3:EGFP)* reporter larvae in *stat3*$^{-/-}$ background display a significant reduction of intestinal EGFP fluorescence at 5 dpf with respect to WT siblings (Fig. 2 E, E'), together with a corresponding 50% reduction of *EGFP* transcripts (Fig. 2

E''). Moreover, to overcome compensation effects present in a genetic mutant and the maternal inherited mRNAs we injected a previously validated translation blocking morpholino (stat3-MO-1) in the *Tg(7xStat3:EGFP)* reporter, using a five-base mismatch morpholino (5mism-MO) as control (Miyagi *et al.,* 2004; Liu *et al.,* 2017; Yamashita *et al.,* 2002). The silencing led to the reduction of the reporter fluorescence to the 25% respect to the 5mism-MO injected fish at 24 hpf and at 48 hpf (Fig. S3 B, B', C, C'); this is consistent with the data obtained with the mutant line at later stages (Fig. 2 D).

In addition, we performed a Fluorescence-activated Cell Sorting (FACS) on dissociated adult intestine and we isolated EGFP-positive and negative cells. Then we performed qRT-PCR to analyse the mRNA levels of *stat3*, *socs3a* and *EGFP* (Fig. 2 C). All these transcripts appear to be significantly upregulated in EGFP-positive cells compared to EGFP-negative ones, thus demonstrating the Stat3 responsiveness of the reporter line.

Taken together, these results highlight that *Tg(7xStat3:EGFP)* transgenic fish are a suitable biosensor for *in vivo* analyses of canonical Stat3 transcriptional activity.

Stat3 pathway is active in proliferating cells during development and in adult intestine

The EGFP expression in *Tg(7xStat3:EGFP)* fish mainly localizes in those tissues that are known to be highly proliferating during zebrafish embryogenesis and larval development. To test whether EGFP-positive cells are involved in proliferative processes, we used EdU to label at 24 and 48 hpf the mitotic cells of *Tg(7xStat3:EGFP)* transgenic fish. The significant co-localization between EdU and EGFP in the haematopoietic niche (Fig. 3 A-A'') and in the Proliferating Tectal Zone (TPZ) of the PML (Fig. 3 B-B''), indicates that Stat3 pathway is indeed active in proliferating cells during zebrafish embryogenesis.

We have previously demonstrated that in zebrafish, during organogenesis, TGFb is a powerful signal for cell cycle arrest (Casari *et al.,* 2014). Hence, we decided to increase the proliferation rate of zebrafish larvae by inhibiting TGFb signalling and test the correlation between increased proliferation and Stat3 responsiveness. To this purpose we treated *Tg(7xStat3:EGFP)* reporter embryos with an inhibitor of TGFb type I receptor (LY364947). As shown in Fig. 3 (C-C''), this stimulus to the cell cycle enhanced the levels of *Tg(7xStat3:EGFP)* fluorescence in the TeO. Consistently, *in situ* hybridization showed a significant increase in the expression of the proliferation marker *pcna* in LY364947

treated larvae when compared to controls (Fig. 3 D-D''). Taken together, these data link, once again, increased proliferation and Stat3 signalling.

The intestinal epithelium represents the most vigorously renewing tissue in mammals as well as in zebrafish (Barker *et al.,* 2007) (Ng *et al.,* 2005). Consistently, *Tg(7xStat3:EGFP)* reporter expression co-localizes with EdU stain in the intestine of 5-dpf larvae (Fig. 4 A-A''). In order to better understand the proliferation dynamics of Stat3 responsive cells, we also performed a Label Retention Assay (Foudi *et al.,* 2009). *Tg(7xStat3:EGFP)* fish have been crossed with the histone-specific *Tg(HSP70:H2B-RFP)* line in order to follow the proliferation-dependent dilution of H2B-RFP nuclear signal in EGFP/Stat3-positive cells. Interestingly, after the first heat shock (HS), that labels in red all larval cells, the rapid loss of nuclear RFP in all intestinal Stat3 positive cells was completed in 48 hpHS. This result demonstrates that Stat3-expressing cells do have an elevated rate of proliferation during intestinal development (Fig. 4 B-B'').

Taken together, these data indicate that during the first days of zebrafish development Stat3 is mainly active in proliferating cells of the haematopoietic tissue, nervous system and intestine.

Stat3 is active in stem-like intestinal cells and needed for normal gut development

When focusing our attention on the adult intestine, we observed that all EGFP-positive cells co-localize with the proliferation marker Pcna, thus confirming that Stat3-responsive intestinal cells retain their mitotic potential until adulthood (Fig. 5 A-A'').

Notably, the self-renewal of the mammalian intestinal epithelium is fuelled by Crypt Base Columnar (CBC) cells, a population of small, adult, undifferentiated, cycling stem cells active at the base of the mammalian crypt in the so called "stem cell zone" (Barker *et al*., 2007) (Cheng and Leblond, 1974). Histological sections show that the anatomy and architecture of adult zebrafish intestinal tract closely resemble those of mammalian small intestine (Ng *et al.,* 2005); while lacking cryptae *sensu stricto*, they have, instead, functionally identical intervillus folds. Transgene expression analysis localizes Stat3 activity in a population of proliferating cells located at the base of the intestinal intervillus folds (Fig. 5 B). To understand the nature of the Stat3-responsive cells we have performed a morphological analysis, based on immunogold labelling, in the intestine of *Tg(7xStat3:EGFP)* adult fish. Using an anti-EGFP antibody, we could observe that Stat3 is active in some intestinal triangular-shaped cells with a global morphology resembling

that of CBC, clearly characterized by a distinctive big dense nucleus that occupies most of the cell body (Fig. 5 C, C').

The transcription factor Sox9 is a known marker for mammalian intestinal stem cells expressed throughout the crypt; notably, its orthologue Sox9b was recently identified in medaka fish intestine as a molecular marker for stem cells at the base of intestinal folds (Formeister *et al.,* 2009; Aghaallaei *et al.,* 2016). To unequivocally identify zebrafish intestinal Stat3-expressing cells as CBC-like, we decided to stain the intestine of *Tg(7xStat3:EGFP)* with antibodies against the transcription factor Sox9b; more than 75% of the intestinal cells expressing EGFP under the control of Stat3 responsive elements also express Sox9b marker in their nuclei (Fig. 5 D). Furthermore the *sox9b* expression levels appear 10-fold higher in *Tg(7xStat3:EGFP)* intestine EGFP-positive cells, compared to EGFP-negative cells (Fig. 5 E). These data suggest that Stat3 pathway operates in a population of zebrafish CBC-like cells that we have named Fold Base Columnar (FBC) cells.

In order to better understand the characteristics of *Tg(7xStat3:EGFP)* intestinal fluorescent cells, we performed qRT-PCR on sorted cells samples and we analysed the expression levels of some well-known intestinal genes: *fabp2*, *pept1* and *agr2* (Fig. 5 E). The protein Fabp2 is a member of intestinal lipid binding proteins (Esteves *et al.,* 2016), it is present in intestinal absorptive cells (Gajda and Storch, 2015). No significant differences on *pept1* and *fabp2* transcript levels were detected between EGFP-positive and EGFP-negative cells, however, *agr2*, reported as a stem cell maker regulated by Wnt/β-catenin canonical signalling pathway (Lamichane *et al*., 2019), appears upregulated in EGFP-positive cells with respect to EGFP-negative ones. These data point out higher levels of Wnt/β-catenin activity and stemness traits in EGFP fluorescent cells. Moreover, we also decided to measure the expression levels of the proliferation markers *pcna* and *cyclinD1* and found an increase in EGFP-positive cells, revealing that they are actively proliferating. Lastly, Notch has been recently identified as a key regulator of stemness in the intestine (Chen *et al*., 2017); we observed an increase of *notch2* transcripts levels in *Tg(7xStat3:EGFP)* intestinal cells compared to *Tg(7xStat3:EGFP)* negative ones, confirming that EGFP-positive cells are intestinal stem cells.

In order to exclude the secretory nature of the fluorescent cells in the gut, we crossed the *Tg(7xStat3:EGFP)* reporter line with the *Tg(nkx2.2a:mEGFP)* transgenic zebrafish line, in which enteroendocrine cells of the intestine are labelled with membrane EGFP (Ng *et al*.,

2005). Interestingly, Stat3-dependent fluorescent cells and Tg*(nkx2.2a:mEGFP)* positive cells are different populations as clearly revealed both by cell counting and morphological analysis under fluorescent confocal microscopy (Fig. S6 A, B). These data show that *Tg(7xStat3:EGFP)* intestinal fluorescent cells are not enteroendocrine cells either, while the morphology of EGFP-positive cells revealed by fluorescent and electron microscopy (Fig. 5 A and C) also excludes the possibility they might be Goblet cells.

In order to assess the requirement of Stat3 for development and maintenance of the intestinal epithelium we have analysed gut formation in *stat3*$^{-/-}$ mutants. The *stat3*^{ia23} allele is genetic lethal, with the humane endpoint reached between 7 and 21 dpf (Fig. 6 A). However, in hundreds of fish screened for homozygosity at later stages, we could observe only two *stat3*$^{-/-}$ mutants surviving until 21 and 52 dpf, respectively (Fig. 6 A, B). For the characterization of genotyped fish, we used a classical histochemical approach focusing on the anatomy of the intestinal epithelium. In general, the most prominent phenotype of mutant larvae is the complete lack of intestinal folds; in particular, the quantitative analysis at 7 dpf shows an incomplete penetrance of this phenotype (about 67% of *stat3*$^{-/-}$ larvae) (Fig. 6 A). However, at 14 dpf, only 50% of survived mutant larvae lack the intestinal folds (Fig. 6 B, C). This finding, combined with the fact that the proportion of *stat3*$^{-/-}$ mutants is decreasing with time (Fig 6 A), suggests that incomplete gut development might be the leading cause of *stat3*$^{-/-}$ mutants mortality. Indeed, the two mentioned survivors (21 and 52 dpf) displayed a normal intestinal mucosa (Fig. 6 B).

Canonical Wnt signalling drives proliferation of Stat3-responsive intestinal cells

It is known that T cell factor 4 (*tcf4,* also known as *tcf7l2*) is a Wnt/β-catenin transducer important in preserving proliferative self-renewal in the zebrafish intestine throughout life (Muncan *et al.,* 2006), alike its murine ortholog (Korinek *et al.,* 1998). In addition, Sox9 in the mammalian intestinal crypts is a direct target of β-catenin/Tcf7l2 (Blache *et al.,* 2004). Furthermore, *Tcf4*$^{hyg/hyg}$ KO mice show the total abrogation of small intestine proliferative cells of the intestinal crypts (van Es *et al*., 2012). Hence, we enquired whether the Stat3 active cells of the zebrafish FBC also depend on β-catenin/Tcf7l2 signalling. To this purpose, we crossed the *Tg(7xStat3:EGFP)* individuals with the *tcf7l2*^{hu892} carriers to generate *Tg(7xStat3:EGFP)* transgenics in a *tcf7l2* mutant background. As shown in Fig. 7, the EGFP level in the Stat3 reporter is almost abolished in the mutants, showing once again that the Stat3-responsive cells in the gut of

Tg(7xStat3:EGFP) are indeed stem cells of the zebrafish intestine. Moreover, we treated *Tg(7xStat3:EGFP)* embryos with XAV, a Wnt/β-catenin inhibitor commonly used in zebrafish (Moro *et al.,* 2012). Interestingly, treating embryos from 48 hpf (before the intestinal organogenesis) to 78 hpf (when the primordial intestinal tube is formed) we found a strong decrease in the activation of the Stat3 reporter line (Fig. 7 C) and, on the other hand, a non-significant decrease in the number of EGFP-positive cells (Fig. 7 C'). Moreover, we performed qRT-PCR analysis on EGFP-positive cells sorted from adult intestines for detection and quantification of the known intestinal Wnt receptors: *fzd5* and *fzd8a* (Nikaido *et al*., 2013). Significantly higher level of expression of these two transcripts, compared to EGFP-negative cells, confirmed the direct responsiveness of EGFP-positive cells to Wnt ligands (Fig. S5 A). These results suggest an important role for Wnt/β-catenin signalling in the intestine, being needed for the maintenance of Stat3 activity in FBC cells but not essential for formation of these cells.

To further investigate the correlation between β-catenin/Tcf7l2 signalling and Stat3, we performed qPCR on 6-dpf *tcf7l2*$^{+/+}$ and *tcf7l2*$^{hu892/hu892}$ larvae and we analysed the gene expression levels of the members of Stat3 pathway (Fig. 7 B). The *tcf7l2*$^{hu892/hu892}$ mutants show an overall downregulation of the pathway: in particular, *jak2b* and *stat3* mRNA levels appear to be significantly downregulated in mutants compared to WT siblings, suggesting a role for β-catenin/Tcf7l2 signalling as a key regulator of Stat3 pathway.

To further study *in vivo* the correlation between Wnt signalling and Stat3-dependent intestinal proliferation, we took advantage of the zebrafish *apc*^{hu745} mutant allele that, being unable to form the β-catenin destruction complex, displays ubiquitous canonical Wnt signalling pathway activation. While *apc*$^{hu745/hu745}$ mutants die before 4 dpf, *apc*$^{hu745/+}$ adults, similarly to the mammalian model, develop, by loss of heterozygosis, spontaneous highly-proliferating adenomatous polyps in the intestine, (Haramis *et al.,* 2006). Notably, when intestinal polyps develop in *apc*^{hu745}*/Tg(7xStat3:EGFP)* mutants, the fish gut displays a significant increase of EGFP fluorescence when compared to normal tissue (Fig. S5B and C). Anti-EGFP immunofluorescence analysis on *apc*^{hu745} intestinal sections shows an enrichment in the number of Stat3-responsive cells within the adenomatous polyps (Fig. 7 D, D' left side), while in normal tissue Stat3 activity is present only in few isolated cells at the base of the intestinal folds (Fig. 7 D, D' right side). Consistently, Pcna proliferation marker is also enriched in adenomatous regions with high Stat3 activity (Fig. 7 D, D"). Notably, co-localization between Stat3 and Pcna reveals that all Stat3-

positive cells have an active cell cycle while Stat3 is active only in a portion of Pcna-expressing cells (Fig. 7 E' and E"). In conclusion, Stat3 activity strictly correlates with proliferation both in normal and adenomatous zebrafish intestines.

Finally, to test whether Stat3 and canonical Wnt signalling are entangled in an autocrine sustaining loop, a feature commonly used by genetic cascades to maintain the stem niche, we treated a Wnt-β-catenin reporter line (Moro *et al*, 2012) with the Jak2 inhibitor AG-490. As shown in supplementary Fig. S5 D, we could not detect a significant effect of Jak2 inhibition on the global levels of canonical Wnt signalling, thus suggesting a one-way signal transduction cascade from Wnt to Stat3.

DISCUSSION

In this work, a Stat3 reporter and a Stat3 CRISPR/Cas9 zebrafish mutant have been generated, validated and analysed to provide a broad view on Stat3 activities and essential functions during early development, tissue homeostasis and pathogenesis. We designed the Stat3 specific reporter cassette based on previous studies performed in mammalian cells, in which a 7x tandem repeat containing the CRP-APRE sequence (TTCCCGAA) from human CRP promoter was shown to respond to IL-6 mediated STAT3 transcription (Zhang *et al.*, 1996). Consistently, the fluorescence of Tg(*7xStat3:EGFP)* reporter is inhibited by Jak2 tyrosine kinase inhibitors and is, instead, activated by injection of either dominant active forms of *stat3* or IL-6 (data not shown). Unexpectedly, although significantly reduced, some fluorescence of Tg(*7xStat3:EGFP)* is maintained also in a Stat3 null background. This might be due to the fact that in the absence of Stat3, and the resultant negative feedback mechanisms activated through Socs1 protein (Liau *et al.,* 2018), Jak2 can phosphorylate other Stat proteins. As a consequence, activated Stats, other than Stat3, can bind Stat3 responsive elements with lower transcriptional efficiency and maintain some EGFP expression as well as activate essential Stat3 target genes. Moreover, the *stat1a* transcript levels appear to be higher in $stat3^{-/-}$ compared to $stat3^{+/+}$ siblings (Fig. S4 D), suggesting an involvement of Stat1a in this possible compensation mechanism. Consistent with this, when the Jak2-mediated activation of Stats is inhibited with AG-490, the EGFP expression of Tg(*7xStat3:EGFP)* is completely abolished.

The Stat3-dependent fluorescence is already detectable in eggs of Tg(*7xStat3:EGFP)* fish. This finding is in agreement with the maternal requirement of Stat3 for embryonic cell proliferation and axis extension at gastrulation (Liu *et al*. 2017). Notably, the early Stat3 transcriptional activity in zebrafish is also consistent with the embryonic lethality of Stat3 null mice (Takeda *et al.,* 1997) and the requirement of LIF/Stat3 for the maintenance of naïve pluripotency in mouse ESC (Carbognin *et al.*, 2016). Moreover, embryos of the stable Tg(*7xStat3:EGFP)* line displays a fluorescent pattern that is significantly overlapping with the zebrafish *stat3* mRNA expression profile previously described by Thisse and colleagues (Thisse et al., 2004). In particular, the Tg(*7xStat3:EGFP)* reporter is active in telencephalon, retina, cranial ganglia, lateral line system, optic tectum, haematopoietic niche and intestine, all tissues where STAT3 has been previously reported to play key roles (Levy and Lee, 2002; Pickert *et al.*, 2009). During organogenesis, the Tg(*7xStat3:EGFP)* reporter activity is particularly elevated in regions with a high proliferative index, such as the larval intestine, the primary hematopoietic tissue and the posterior region of the optic tectum. In all these regions, the Stat3-positive cells are themselves actively proliferating as demonstrated by label retention assay, co-localization with Pcna and EdU labelling. The fact that these actively proliferating tissues express high levels of Stat3 is indeed in agreement with the well-known oncogenic activity of STAT3 in glioblastoma, colorectal cancer and leukemia (Sherry *et al.*, 2009; Corvinus *et al*., 2005; Benekli *et al.*, 2002).

Stat3 responsiveness in the adult intestine is located in a restricted population of actively proliferating cells identified as FBC cells; remarkably, FBC cells express the stem cell specific marker Sox9b and display a stem cell-like morphology. These findings are strongly consistent with STAT3 activity being absolutely required in mice for small-intestine crypt stem cell survival at both the +4 to +6 label-retaining and crypt base columnar cell locations (Matthews et al., 2011). On the other side, it is known that mice carrying conditional ablation of STAT3 in differentiated intestinal epithelial cells develop normally (Pickert *et al*., 2009). Hence, mouse and zebrafish findings are totally compatible with the hypothesis that STAT3 is required for survival and expansion of intestinal progenitors. Notably, both the AG-490 treatment and *stat3*^{ia23} mutation lead to a severe impairment of intestine development that might well be the cause for loss of all *stat3*$^{ia23/ia23}$ animals before the third week of age. Thus, slightly different from what

observed by Liu et al. (2017) in their zebrafish *stat3* KO mutant, our results would drive to the conclusion that Stat3 is needed for early larval development, being functionally conserved and needed for gut development and maintenance. The highly proliferating sox9b-positive and Stat3-responsive cells of zebrafish intestine require TCF/β-catenin for their development and are extremely expanded in number in intestinal adenomas of *apc* mutant fish, hence indicating that STAT3 responsiveness and their consequence in the gut are under control of the TCF/β-catenin signalling pathway. Moreover, the fact that STAT3 responsive cells of zebrafish intestinal adenomas represent only a fraction of the proliferating population suggests that they might be intestinal cancer stem cells, thus denoting Stat3 as a stemness marker in normal and neoplastic intestine and the Jak2 kinase as a suitable therapeutic target in CRC.

MATERIAL AND METHODS

Animals husbandry and lines

Animals were staged and fed as described by Kimmel I (1995) and maintained in large scale aquaria system.

Embryos were obtained by natural mating, raised at 28 °C in Petri dishes containing fish water (50X: 25 g Instant Ocean, 39.25 g $CaSO_4$ and 5 g $NaHCO_3$ for 1 L) and kept in a 12:12 light-dark (LD) cycle. All experimental procedures complied with European Legislation for the Protection of Animals used for Scientific Purposes (Directive 2010/63/EU).

apc^{hu745} (Haramis *et al.*, 2006) mutant carriers were genotyped by PCR amplification and sequencing. *Tg(HSP70:H2B:mRFP)* transgenic line was a kind gift of the Meyer Lab (Institute of Molecular Biology, Leopold-Franzens-University Innsbruck). The *Tg(gata1:dsRed)*^{sd2} transgenics and *Tg(nkx2.2a:mEGFP)* transgenic lines and *tcf4*^{hu892} (*tcf4*$^{exl/exl}$) mutants are described in Traver *et al.,* (2003), Ng *et al.,* (2005) and Muncan *et al*., (2006), respectively. The *Tg(7xTCF-Xla.Siam:nlsmCherry)*^{ia5} reporter zebrafish line is described in Moro *et al.,* 2012. All animal experiments were performed under permission of the ethical committee of the University of Padova and the Italian Ministero della Salute (23/2015-PR).

Generation of Tg(7xStat3-Hsv.Ul23:EGFP) reporter and stat3 ^{ia23} mutant.

The Stat3 responsive promoter sequence, containing the seven tandem repeats from the promoter of the human C-reactive protein (CRP) (nucleotides -123 to -85), was obtained in the form of the pLucTKS3 plasmid, a kind gift of Prof. Jiayuh Lin (The Ohio State University Comprehensive Cancer Center, Columbus, Ohio). The promoter fragment, containing the Stat3 responsive elements (SRE) and the TK minimal promoter, was isolated from the pLucTKS3 plasmid using HindIII and SacII restriction enzymes and subcloned into the Gateway 5' entry vector pME-MCS (Invitrogen). The resulting p5E-TKS3 entry vector was recombined together with the EGFP-carrying middle entry vector and the p3E-polyA entry clone, into the Tol2 destination vector pDestTol2pA2 (Invitrogen) as already described by (Kwan *et al.,* 2007). 30 pg of the recombined Tol2 destination vectors with 25 pg of *in vitro* synthesized Tol2 transposase mRNA (Kawakami *et al.,* 2004) were co-injected into one cell-stage wild-type zebrafish embryos. Microinjected embryos were selected at 24 hpf for their elevated mosaic transgenic expression using an epifluorescent microscope, raised to adulthood and outcrossed to wild-type fish. The F_1 founders were finally selected for fluorescence level and Mendelian segregation of their transgene in order to establish single allele transgenic lines named *Tg(7xStat3-Hsv.Ul23:EGFP)*.

stat3^{ia23} zebrafish mutants were generated by CRISPR/Cas9-mediated genome editing. A single guide RNA (sgRNA) was designed using the CHOPCHOP software https://chopchop.rc.fas.harvard.edu, to specifically target an optimal CRISPR sequence on exon 14 of *stat3* gene (NM 131479). The *stat3*-targeting sgRNA, (with the specific targeting sequence GGTCGATCTTAAGTCCTTGG-ngg), was generated according to Gagnon *et al.* (2014) and transcribed *in vitro* using the MEGAshortscript T7 kit (Life Technologies, AM1354).

One-cell stage embryos were injected with 2 nL of a solution containing 280ng/uL Cas9 protein (M0646, Bio Labs) and 68 ng/uL sgRNA; Phenol Red was used as injection marker. F_0 injected embryos were raised to adulthood and screened, by genotyping the F_1, for germline transmission of the mutation. Heterozygous mutants harbouring the mutation were then outcrossed 4 times and then incrossed to obtain homozygous mutants (F_5 generation).

stat3^{ia23} heterozygous and homozygous mutants were identified by loading in agarose gel the product of the PCR performed using the following primers: *stat3*-Fw (5'-GGCCTCTCTGATAGTGACCG-3'), *stat3*-Rv (5'-AGTTGTGCTTAGACGCGATC-3').

Organ dissection

To analyse the reporter signal in the adult, *Tg(7xStat3-Hsv.Ul23:EGFP)* fish were euthanized and dissected under the epifluorescence microscope. The intestine and other organs belonging to the gastro urinary tract were imaged immediately after, either *in situ* or isolated, with conventional fluorescence or confocal microscopy. Isolated intestine from *Tg(7xStat3-Hsv.Ul23:EGFP)/apc*$^{+/-}$ and *Tg(7xStat3-Hsv.Ul23:EGFP)* 12mpf zebrafish were dissected in PBS solution and then fixed in 4% PFA in PBS for either paraffin embedding, cryosectioning and further immunolabeling.

Immunofluorescence, Immunogold labelling and TEM analysis

Immunofluorescence staining on sections of 6 mpf *Tg(7xStat3-Hsv.Ul23:EGFP)/apc*$^{+/-}$ intestines was performed as previously described by Schiavone *et al.* (2014) using chicken anti-EGFP antibody (A10262, Life Technologies)(1:250); mouse anti-PCNA (M0879, Dako) (1:100); anti-chicken-Alexa488 (A-11039, Life Technologies)(1:500); anti-mouse-TRITC (1:500) (R 0270, Dako). Cryosectioning and immunofluorescence analysis of 6-mpf *Tg(7xStat3-Hsv.Ul23:EGFP)* intestines were performed as described by Zhang *et al*. (2017) using goat anti-zSox9b (Zebrafish) (ER14-1692, RayBiotech)(1:100). Whole mount immunofluorescence staining on zebrafish larvae injected with CMV-mStat3C plasmid, 24-hpf larvae were fixed with PFA 4% for 2 hours at room temperature and stored at -20°C in methanol. After rehydration, larvae were washed with 150 mM Tris-HCl (pH 9) for 5 minutes. Then the samples were incubated at 70°C for 15 minutes. After 2 5-minute long washes in PBS 1% Triton, larvae were permeabilized with acetone for 20 minutes at -20°C. Acetone was removed with two washes in deionized water and 2 washes in PBS 1% Triton. Epitopes were blocked for two hours with PBS 1% Triton, 1% BSA, 2% goat serum. Samples were then incubated with primary antibody anti-STAT3 mouse monoclonal (1:75) (Cell Signalling, 9139) for 72 hours. After a brief wash in PBS 1% Triton, samples were washed two times with PBS 1% Triton 5% goat serum for 1 hour. After over-night incubation of the samples with secondary antibody (anti-mouse Alexa 488, Life Technologies), larvae were washed two times with PBS 1% Triton 5%

goat serum for 1 hour and 3 times with PBS 0.5% Triton for 10 minutes.

Immunogold labelling was performed on adult *Tg(7xStat3-Hsv.Ul23:EGFP)/apc*$^{+/-}$ zebrafish intestine using the chicken anti-EGFP (1:25)(A10262, Life Technologies) primary antibody and anti-chicken-(10nm) Au secondary antibody (25429, EMS). TEM acquisitions were performed using a FEI Tecnai G2 microscopy and a TVIPS F114 bottom-mounted camera.

Drug treatments

The following chemical compounds were used: AG-490 (T3434, Sigma); LLL12 (573131, Calbiochem); LY-364947 (L6293, Sigma); XAV939 (X3004, Sigma). All drugs were dissolved in DMSO, stored in small aliquots and kept in the dark at -20°C. *Tg(7xStat3-Hsv.Ul23:EGFP)* embryos were dechorionated and exposed to drugs diluted in fish water. 2 mM 1-phenyl-2-thiourea (PTU) was used to inhibit pigmentation. 100 µM AG-490 treatment was performed from 24 to 48 hpf, 60 µM AG-490 was delivered in 3-6 dpf treatments, 80 µM AG-490 was administered from 8 to 72 hpf. 0.025 µM LLL12 solution was provided from 24-48 hpf. 60 µM LY-364947 treatment was performed from 24 to 48 hpf. 10 µM XAV939 treatment was performed from 48-78 hpf.

Proliferation assays

EdU proliferation assay was performed using the Click-iT® EdU Alexa Fluor® 594 Imaging Kit (Thermo Fisher Scientific) following manufacturers instruction. After initial exposure to EdU reagent, *Tg(7xStat3-Hsv.Ul23:EGFP)* 48-hpf embryos and 4 dpf-larvae were kept in fish water for respectively 1h 30' and 24 h. Proliferating cells were later on stained with Alexa 594 red fluorophore and fixed in 4% PFA in PBS. Label retention assay was performed using the *Tg(HSP70:H2B:mRFP)* transgenic line. Offspring was heat-shocked at 4 dpf by replacing the fish water with water preheated to 42 °C and afterwards incubating the larvae in an air incubator at 37 °C for 1 hour. The larvae were then analysed under the epifluorescent microscope for nuclear RFP and STAT3:EGFP fluorescence. Samples were mounted on a depression slide and monitored at 6 hours post heat shock (hpHS), 24 hpHS and 48 hpHS to observe the dilution of the nuclear staining using a Nikon C2 confocal microscope.

In situ hybridization

Whole mount RNA *in situ* hybridization on zebrafish embryos was performed as described by Thisse *et al.* (2014) and stained with NBT/BCIP staining solution (Sigma, 11681451001). It is worth mentioning that treated and control embryos were hybridized together as the control embryos had the tip of the tail cut for their *post hoc* recognition. *EGFP* probe was synthesized from the pME-*EGFP* plasmid supplied by the Tol2 kit (Invitrogen). *pcna* probe was obtained as described by Baumgart *et al.* (2014).The intensity of *in situ* hybridization signals was quantified after image segmentation based on colour hue, saturation and intensity using ImageJ software.

mRNA isolation and quantitative real time reverse transcription PCR (qRT-PCR)

For expression analysis, RNA was extracted from pools of 15 larvae at 7 dpf with TRIzol reagent (Thermo Fisher Scientific, 15596018). Total mRNA was treated with RQ1 RNase-Free DNase (Promega, M6101) and then used for cDNA synthesis with random primers (Promega, C1181) and M-MLV Reverse Transcriptase RNase H (Solis BioDyne, 06-21-010000) according to the manufacturer's protocol. qPCRs were performed in triplicate with CybrGreen method using a Rotor-gene Q (Qiagen) and the 5x HOT FIREPol EvaGreen qPCR Mix Plus (Solis BioDyne, 08-36-00001); *z-gapdh* was used as internal standard in each sample. The cycling parameters were: 95 °C for 14 min, followed by 45 cycles at 95 °C for 15 s, 60 °C for 35 s, and 72°C for 25 s. Threshold cycles (Ct) and melting curves were generated automatically by Rotor-Gene Q series software. Ct values were divided for *z-gapdh* Ct values in order to obtain dCt values. As reporter in Livak and Schmittgen (2001), one dCt was identified as reference dCt and it was subtracted to dCt of other samples: with this procedure we obtained ddCt. Results (R) were obtained with the following formula: $R=2^{ddCt}$. Sequences of specific primers used in this work for qRT-PCR and RT-PCR are listed in supplementary material Table 1. Primers were designed using the software Primer 3 (http://bioinfo.ut.ee/primer3-0.4.0/input.htm).

Imaging

For *in vivo* imaging, transgenic embryos and larvae were anesthetized with 0.04% tricaine, embedded in 0.8% low-melting agarose and mounted on a depression slide. The Nikon C2 confocal system was used to acquire fluorescence images from embryos, larvae and immunofluorescences on slides. For *Tg(gata1:dsRed)sd2/ Tg(7xStat3-Hsv.Ul23:EGFP)* fish images were acquired using a Leica SP5 confocal microscope. Samples from *in situ* hybridization were mounted in 87% glycerol, then observed with a Leica M165 FC microscope equipped with a Nikon DS-Fi2 digital camera. Histological sections after hematoxylin/eosin staining were photographed on a Leica DMR using a Nikon DS-Fi2 digital camera. All images were analysed with Fiji (ImageJ) software and the integrated density of fluorescence was calculated setting a standard threshold on non fluorescent embryos.

The VIBE-Z software (Ronneberger, 2012) was used to visualize single planes of the brain of 72-hpf *Tg(7xStat3-Hsv.Ul23:EGFP)* transgenic line.

Fluorescence-Activated Cell Sorting (FACS)

Tg(7xStat3-Hsv.Ul23:EGFP) intestines were cut longitudinally in PBS and then were scraped in order to separate intestinal luminal cells from intestinal muscular tissue. Intestinal cells were treated with collagenase 2.2mg/ml, trypsin 0,25mg/ml and EDTA 1 mM in sterile PBS for 5 minutes and mechanically dissociated every minute. Dissociation was blocked adding $CaCl_2$ 1 mM and 10% FBS. Cell suspension was filtered with 100 µm cell strainer. After centrifugation at 800 xg for 5 minutes, samples were resuspended in 200 µl of trypsin 0.25 mg/ml and 1 mM EDTA in PBS and filtered through a 40 µm cell strainer. Then cells were centrifuged at 800 xg for 5 minutes and resuspended in 100 µl in sterile PBS with 1% FBS, streptomycin 1X, 1 mM EDTA. For sorting we used FACS Aria IIIu sorter (BD Biosciences, San José, USA) with the following settings for EGFP: argon-ion Innova Laser (Coherent, USA) (488 nm, 100 mW); 100 µM nozzle; sorting speed 500 events/s in 0-32-0 sort precision mode. We performed data acquisition and analysis with the BD FACSDiva software (BD Biosciences, San José, CA, USA).

Statistical analysis

Statistical analysis was performed using Graph Pad Prism software V6.0. Data are presented as the means ± SEM. Comparison between different groups of samples was performed by Student's t-test with a confidence interval of 95%. The p-values are indicated with asterisks: *, $p< 0.05$; **, $p< 0.01$; ***, $p< 0.001$; ****,$p<0.0001$.

Acknowledgements

We would like to thank Drs. Luigi Pivotti, Martina Milanetto, Carlo Zatti and Ludovico Scenna for their professional help in managing the Padua Zebrafish Facility as well as Prof. Wolfgang Driever and dr. Saskia Lindner at the University of Freiburg for their great help in VIBE-Z acquisitions and analysis. The work was supported by AIRC grant IG 2017 19928, by European Union Grant ZF-HEALTH CT-2010-242048 and by Teaching Staff Mobility grants in the framework of University of Padova / University of Freiburg bilateral agreements.

REFERENCES

Aghaallaei N., Gruhl F., Schaefer C. Q., Wernet T., Weinhardt V., Centanin L., Loosli F., Baumbach J., Wittbrodt, J. (2016). Identification, visualization and clonal analysis of intestinal stem cells in fish. *Development* (Cambridge, England)**, 143(19),** 3470–3480.

Ahmad R., Kumar B., Chen Z., Chen X., Müller D., Lele S.M., Washington M.K., Batra S.K., Dhawan P., Singh A.B. (2017). Loss of claudin-3 expression induces IL6/gp130/Stat3 signaling to promote colon cancer malignancy by hyperactivating Wnt/β-catenin signaling. *Oncogene.* **36(47):**6592-6604.

Barker N., van Es J. H., Kuipers J., Kujala P., van den Born M., Cozijnsen M., Haegebarth A., Korving J., Begthel H., Peters P. J. *et al.* (2007). Identification of Stem Cells in Small Intestine and Colon by Marker Gene Lgr5. *Nature* **449,** 1003-1007.

Baumgart M., Groth M., Priebe S., Savino A., Testa G., Dix A., Ripa R., Spallotta F., Gaetano C., Ori M. *et al.* (2014). RNA-seq of the aging brain in the short-lived fish N. furzeri – conserved pathways and novel genes associated with neurogenesis. *Aging Cell.* **13**: 965–974.

Benekli M., Xia Z., Donohue K.A., Ford L.A., Pixley L.A., Baer M.R., Baumann H., Wetzler M. (2002). Constitutive activity of signal transducer and activator of transcription 3 protein in acute myeloid leukemia blasts is associated with short disease-free survival. *Blood.* **99(1):**252-7.

Blache P., van de Wetering M., Duluc I., Domon C., Berta P., Freund J.N., Clevers H., Jay P. (2004). SOX9 is an intestine crypt transcription factor, is regulated by the Wnt pathway, and represses the CDX2 and MUC2 genes. *J Cell Biol.* **166(1):**37-47.

Carbognin E., Betto R.M., Soriano M.E., Smith A.G., & Martello G. (2016). Stat3 promotes mitochondrial transcription and oxidative respiration during maintenance and induction of naive pluripotency. *The EMBO Journal.* **35:**618–634.

Casari A, Schiavone M, Facchinello N, Vettori A, Meyer D, Tiso N, Moro E, Argenton F. (2014). A Smad3 transgenic reporter reveals TGF-beta control of zebrafish spinal cord development. *Dev Biol*. **396(1)**:81-93.

Chen K., Srinivasan T., Tung K., Belmonte J.M., Wang L., Murthy P.K.L., Choi J., Rakhilin N., King S., Varanko A.K. *et al.* (2017) A Notch positive feedback in the intestinal stem cell niche is essential for stem cell self-renewal. *Mol Syst Biol.* **13:** 927

Cheng, H. and Leblond, C. P. (1974). Origin, Differentiation and Renewal of the Four Main Epithelial Cell Types in the Mouse Small Intestine. V. Unitarian Theory of the Origin of the Four Epithelial Cell Types. *Am. J. Anat.* **141,** 537-561.

Chung, Y.J., Park, B.B., Kang, Y.J., Kim, T.M., Eaves, C.J., Oh, I.H. (2006). Unique effects of Stat3 on the early phase of hematopoietic stem cell regeneration. *Blood*. **108(4)**,1208-15.

Corvinus F.M., Orth C., Moriggl R., Tsareva S.A., Wagner S., Pfitzer E.B., Baus D., Kaufmann R., Huber L.A., Zatloukal K. *et al.* (2005). Persistent STAT3 activation in colon cancer is associated with enhanced cell proliferation and tumor growth. *Neoplasia.* **7(6):**545-55.

Esteves A., Knoll-Gellida A., Canclini L., Silvarrey M.C., Andrè M., Babin P.J. (2016). Fatty acid binding protein have the potential to channel dietary fatty acids into enterocyte nuclei. *J Lipid Res*. **57(2):** 219-232.

Formeister E.J., Sionas A.L., Lorance D.K., Barkley C.L., Lee G.H., Magness S.T. (2009). Distinct SOX9 levels differentially mark stem/progenitor populations and enteroendocrine cells of the small intestine epithelium. *Am J Physiol Gastrointest Liver Physiol.* **296(5):**G1108-18.

Foudi A., Hochedlinger K., Van Buren D., Schindler J. W., Jaenisch R., Carey V. and Hock H. (2009). Analysis of Histone 2B-GFP Retention Reveals Slowly Cycling Hematopoietic Stem Cells. *Nat. Biotechnol.* **27,** 84-90.

Gagnon J.A., Valen E., Thyme S.B., Huang P., Akhmetova L., Pauli A., Montague T.G., Zimmerman S., Richter C., Schier A.F. (2014). Efficient mutagenesis by Cas9 protein-mediated oligonucleotide insertion and large-scale assessment of single-guide RNAs. *PLoS One.* **9(5):**e98186.

Gajda A.M., Storch J. (2015). Enterocyte Fatty Acid Binding Proteins (FABPs): different functions of liver- and intestinal-FABPs in the intestine. *Prostaglandins Leukot Essent Fatty Acids*. **93**: 9-16.

Gallardo V.E., and Behra M. (2013). Fluorescent Activated Cell Sorting (FACS) Combined with Gene Expression Microarrays for Transcription Enrichment Profiling of Zebrafish Lateral Line Cells. *Methods.* **62(3):** 226–231.

Galoczova M., Coates P., Vojtesek B. (2018). STAT3, stem cells, cancer stem cells and p63*. Cell Mol Biol Lett.* **23:**12.

Haramis, A.-P. G., Hurlstone, A., van der Velden, Y., Begthel, H., van den Born, M., Offerhaus, G. J. A., & Clevers, H. C. (2006). Adenomatous polyposis coli-deficient zebrafish are susceptible to digestive tract neoplasia. *EMBO Reports,* **7(4)**, 444–449.

Huynh J., Chand A., Gough D., Ernst M. (2019). Therapeutically exploiting STAT3 activity in cancer - using tissue repair as a road map. *Nat Rev Cancer.* **19(2):**82-96.

Johnson D.E., O'Keefe R.A., & Grandis J.R. (2018). Targeting the IL-6/JAK/STAT3

signalling axis in cancer. *Nature Reviews Clinical Oncology.* **15:**234–248.

Kawakami K., Takeda H., Kawakami N., Kobayashi M., Matsuda N., Mishina M. (2004). A transposon-mediated gene trap approach identifies developmentally regulated genes in zebrafish. *Dev Cell.* **7(1):**133-44.

Kimmel, C. B., Ballard, W. W., Kimmel, S. R., Ullmann, B. and Schilling, T. F. (1995). Stages of embryonic development of the zebrafish. *Dev. Dyn*. **203:** 253–310.

Korinek V., Barker N., Moerer P., van Donselaar E., Huls G., Peters P.J., Clevers H. (1998). Depletion of epithelial stem-cell compartments in the small intestine of mice lacking Tcf-4. *Nat Genet.* **19(4):**379-83.

Kwan, K. M., Fujimoto, E., Grabher, C., Mangum, B. D., Hardy, M. E., Campbell, D. S., Parant, J. M., Yost, H. J., Kanki, J. P. and Chien, C. B. (2007). The Tol2kit: A Multisite Gateway-Based Construction Kit for Tol2 Transposon Transgenesis Constructs. *Dev. Dyn.* **236,** 3088-3099.

Lamichane B.D., Jung S.Y., Yun J., Kang S., Kim D. Y., Lamichane S., Kim Y. J., Park J.H., Jang W.B., Ji S.T. *et al.* (2019). AGR2 is a target of canonical Wnt/β-catenin signaling and is important for stemness maintenance in colorectal cancer stem cells. *Biochem. Biophys. Res. Commun.* **515(4):** 600-606

Levy D.E., Lee C.K. (2002). What does Stat3 do? *J Clin Invest.* **109(9):**1143-8.

Lin, L., Hutzen, B., Li, P. K., Ball, S., Zuo, M., DeAngelis, S., Foust, E., Sobo, M., Friedman, L., Bhasin, D. et al. (2010). A Novel Small Molecule, LLL12, Inhibits STAT3 Phosphorylation and Activities and Exhibits Potent Growth-Suppressive Activity in Human Cancer Cells. *Neoplasia* **12,** 39-50.

Liau N.P.D., Laktyushin A., Lucet I.S., Murphy J.M., Yao S., Whitlock E., Callaghan K., Nicola N.A., Kershaw N.J., Babon J.J. (2018). The molecular basis of JAK/STAT inhibition by SOCS1. *Nature Commun.* **9(1):**1558.

Livak K.J., Schmittgen T.D. (2001) Analysis of relative gene expression data using real-time quantitative PCR and the 2(-Delta Delta C(T)) Method. *Methods.* **25(4)**:402–408.

Liu Y., Sepich D.S., Solnica-Krezel L. (2017). Stat3/Cdc25a-dependent cell proliferation promotes embryonic axis extension during zebrafish gastrulation. *PLoS Genet.* **13(2):** e1006564.

Matthews J.R., Sansom O.J., Clarke A.R. (2011). Absolute requirement for STAT3 function in small-intestine crypt stem cell survival. *Cell Death Differ.* **18(12):**1934-43.

Meydan N., Grunberger T., Dadi H., Shahar M., Arpaia E., Lapidot Z., Leeder J. S., Freedman M., Cohen A., Gazit A. et al. (1996). Inhibition of Acute Lymphoblastic

Leukaemia by a Jak-2 Inhibitor. *Nature* **379,** 645-648.

Miyagi C., Yamashita S., Ohba Y., Yoshizaki H., Matsuda M., Hirano T. STAT3 noncell-autonomously controls planar cell polarity during zebrafish convergence and extension. (2004). J. *Cell Biol*. **166(7)**:975–81.

Morin P.J., Sparks A.B., Korinek V., Barker N., Clevers H., Vogelstein B., Kinzler K.W. (1997). Activation of beta-catenin-Tcf signaling in colon cancer by mutations in beta-catenin or APC. *Science*. **275:**1787–1790.

Moro. E., Ozhan-Kizil, G., Mongera, A., Beis, D., Wierzbicki, C., Young, R. M., Bournele, D., Domenichini, A., Valdivia, L. E., Lum, L. et al. (2012). In Vivo Wnt Signaling Tracing through a Transgenic Biosensor Fish Reveals Novel Activity Domains. *Dev. Biol.* **366,** 327-340.

Moro E., Vettori A., Porazzi P., Schiavone M., Rampazzo E., Casari A., Ek O., Facchinello N., Astone M., Zancan I. *et al.* (2013). Generation and application of signaling pathway reporter lines in zebrafish. *Mol Genet Genomics.* **288(5-6):**231-42.

Muncan V., Sansom O.J., Tertoolen L., Phesse T.J., Begthel H., Sancho E., Cole A.M., Gregorieff A., de Alboran I.M., Clevers H. *et al.* (2006). Rapid loss of intestinal crypts upon conditional deletion of the Wnt/Tcf-4 target gene c-Myc. *Mol Cell Biol.* **26(22):**8418-26.

Ng A. N., de Jong-Curtain T. A., Mawdsley D. J., White S. J., Shin J., Appel B., Dong P. D., Stainier D. Y. and Heath J. K. (2005). Formation of the Digestive System in Zebrafish: III. Intestinal Epithelium Morphogenesis. *Dev. Biol.* **286,** 114-135.

Nikaido M., Law E.W.P., Kelsh R.N. (2013). A Systematic Survey of Expression and Function of Zebrafish *frizzled* Genes. *PLos One.* **8(1):**e54833

Pattabiraman D.R., Weinberg R.A. (2014). Tackling the cancer stem cells - what challenges do they pose? *Nat Rev Drug Discov.* **13(7):**497-512.

Pickert G., Neufert C., Leppkes M., Zheng Y., Wittkopf N., Warntjen M., Lehr H.A., Hirth S., Weigmann B., Wirtz S. *et al.* (2009). STAT3 links IL-22 signaling in intestinal epithelial cells to mucosa wound healing. *J Exp Med.* **206(7):**1465-72.

Raz R., Lee C.K., Cannizzaro L.A., d'Eustachio P., Levy D.E. (1999). Essential role of STAT3 for embryonic stem cell pluripotency. *Proc Natl Acad Sci U S A.* **96(6):**2846-51.

Recher G., Jouralet J., Brombin A., Heuzé A., Mugniery E., Hermel J.M., Desnoulez S., Savy T., Herbomel P., Bourrat F. *et al.* (2013). Zebrafish midbrain slow-amplifying progenitors exhibit high levels of transcripts for nucleotide and ribosome biogenesis. *Development.* **140(24):**4860-9.

Ronneberger O., Liu K., Rath M., Rueß D., Mueller T., Skibbe H., Drayer B., Schmidt T., Filippi A., Nitschke R. *et al.* (2012). ViBE-Z: a framework for 3D virtual colocalization analysis in zebrafish larval brains. *Nat Methods.* **9(7):**735-42.

Schiavone M., Rampazzo E., Casari A., Battilana G., Persano L., Moro E., Liu S., Leach S.D., Tiso N., Argenton F. (2014). Zebrafish reporter lines reveal in vivo signaling pathway activities involved in pancreatic cancer. *Dis Model Mech.* **7(7):**883-94.

Sellier H., Rébillard A., Guette C., Barré B., Coqueret O. (2013). How should we define STAT3 as an oncogene and as a potential target for therapy? *JAKSTAT.* **2(3):**e24716.

Sherry M.M., Reeves A., Wu J.K., Cochran B.H. (2009). STAT3 is required for proliferation and maintenance of multipotency in glioblastoma stem cells. *Stem Cells.* **27(10):**2383-92.

Takeda K., Nogushi K., Shi W., Tanaka T., Matsumoto M., Yoshida N., Kishimoto T., Akira S. (1997). Targeted disruption of the mouse Stat3 gene leads to early embryonic lethality. *Proc Natl Acad Sci U S A.* **94(8):**3801-4.

Thisse B., Heyer V., Lux A., Alunni V., Degrave A., Seiliez I., Kirchner J., Parkhill J.P., Thisse C. (2004). Spatial and temporal expression of the zebrafish genome by large-scale in situ hybridization screening. *Methods Cell Biol.* **77:**505-19.

Thisse B., Thisse C. (2014). In situ hybridization on whole-mount zebrafish embryos and young larvae. *Methods Mol Biol.* **1211:**53-67.

Traver D., Paw B.H., Poss K.D., Penberthy W.T., Lin S., Zon L.I. (2003). Transplantation and in vivo imaging of multilineage engraftment in zebrafish bloodless mutants. *Nat Immunol.* **4(12):**1238-46.

Turkson J., Bowman T., Garcia R., Caldenhoven E., De Groot R.P., Jove R. (1998). Stat3 activation by Src induces specific gene regulation and is required for cell transformation. *Mol Cell Biol.* **18(5):**2545-52.

Van Es J., Haegebarth A., Kujala P., Itkovitz S., Koo B., Boj SF., Korving J., van den Born M., van Oudenaarden A., Robine S. *et al.* (2012). A critical role of Wnt effector Tcf4 in adult intestinal homeostatic self-renewal. *Mol. Cell. Biol.* **40(10)**:1918-27

Vu T., Datta P.K. (2017). Regulation of EMT in Colorectal Cancer: A Culprit in Metastasis. *Cancers*. **9(12):** 171.

Wang S.W., Sun Y.M. (2014). The IL-6/JAK/STAT3 pathway: potential therapeutic strategies in treating colorectal cancer (Review). *Int J Oncol.* **44(4):**1032-40.

Yamashita S., Miyagi C., Carmany-Rampey A., Shimizu T., Fujii R., Schier A.F., et al. (2002). Stat3 controls cell movements during Zebrafish gastrulation. *Dev. cell.*; **2(3)**:363–75.

Zhang D., Sun M., Samols D., Kushner I. (1996). STAT3 participates in transcriptional activation of the C-reactive protein gene by interleukin-6. *J Biol Chem.* **271(16):**9503-9.

Zhang H., Wen W., Yan J. (2017). Application of immunohistochemistry technique in hydrobiological studies. *Aquac Fish*. **2:**140–144.

Figures

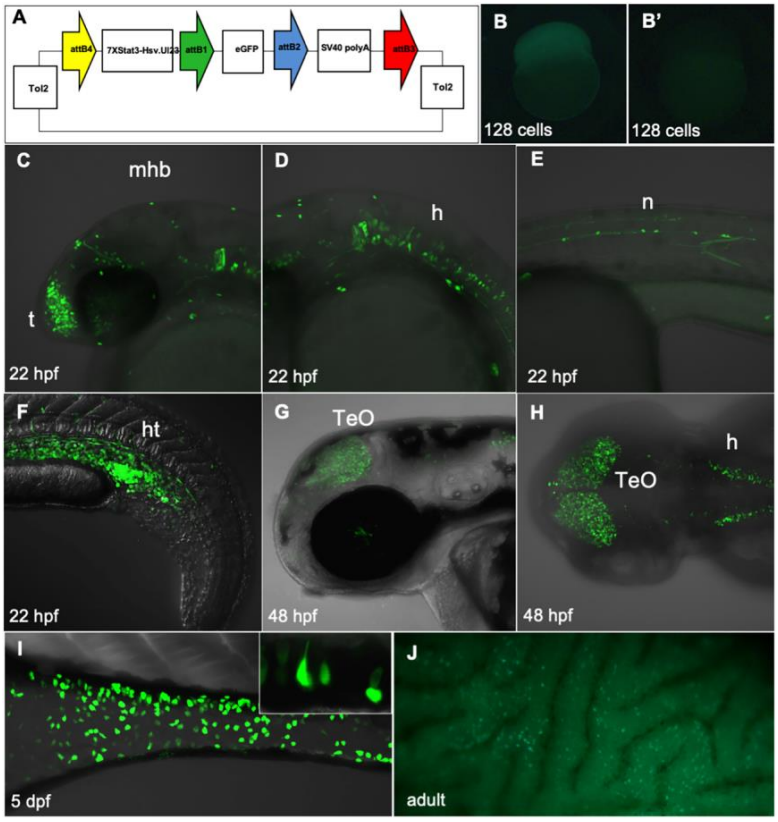

Fig. 1 : Generation of *Tg(7xStat3-Hsv.Ul23:EGFP)* and characterization of their expression pattern. A: Schematic representation of the Tol-2 vectors used to generate the *Tg(7xStat3-Hsv.Ul23:EGFP)*. B-B': Diffused EGFP is detectable in early stage embryos obtained by outcrossing transgenic females (B), not with transgenic males (B'). C-F: At 22 hpf, EGFP expression is detectable in the anterior telencephalic region (t), the primordial midbrain hindbrain boundary (mhb), the hindbrain (h), the primitive neuromasts (n) and in the haematopoietic tissue (ht). G-H: At 48 hpf EGFP expression is mostly located in the optic tectum (TeO) and in the hindbrain (h). I-J: Starting from 4 dpf EGFP expression is detectable in the developing intestine in isolated pear-shaped cells (I); the intestinal fluorescence lasts throughout adulthood (J).

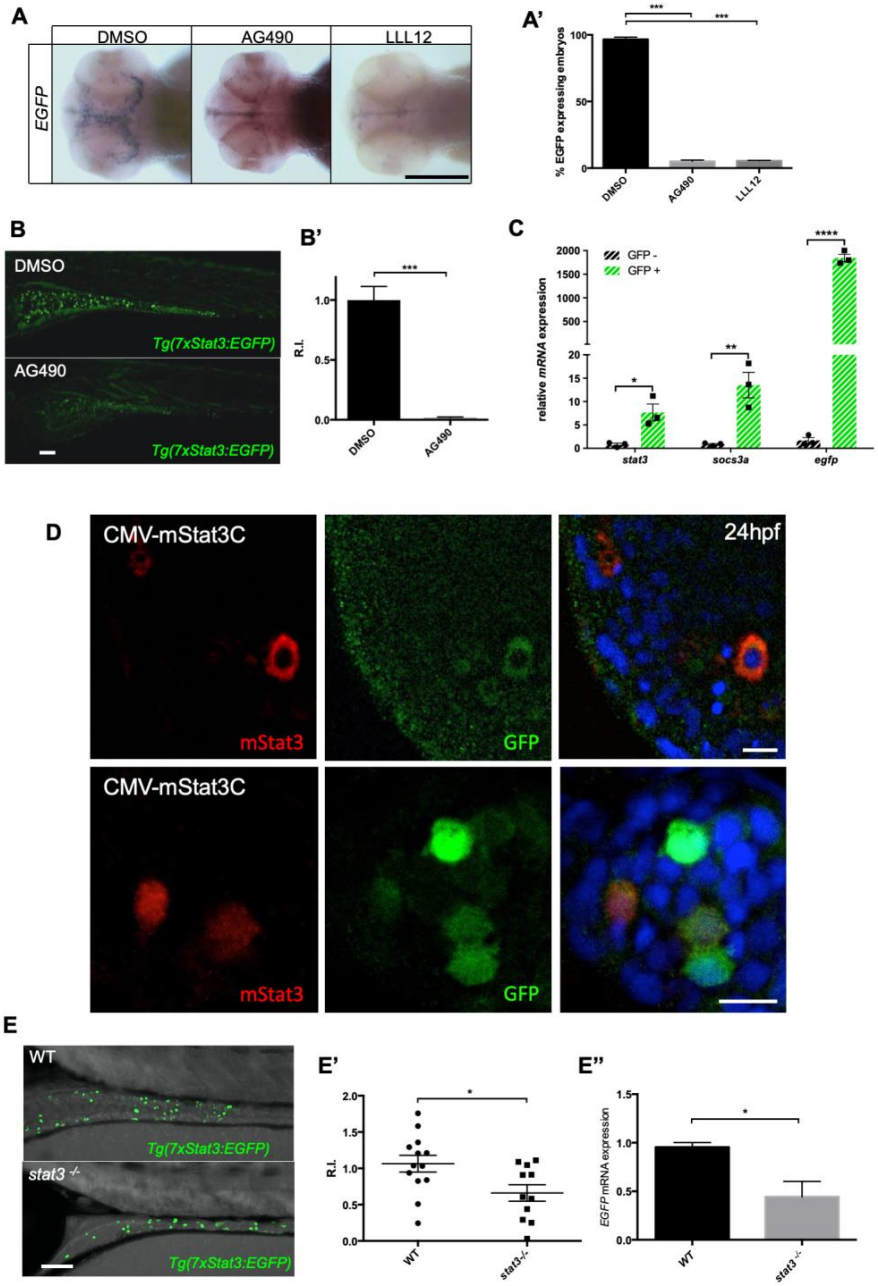

Fig. 2 : The *Tg(7xStat3:EGFP)* is a *bona fide* Stat3 pathway reporter. A: Whole mount *in situ* hybridization detection of *EGFP* mRNA in the optic tectum of 48-hpf embryos treated with the inhibitors of Stat3 pathway AG-490 and LLL12; control embryos were treated with DMSO. Scale bar: 100µm. A': Graphical representation of the percentage of samples displaying *EGFP* mRNA expression in the optic tectum. Statistical analysis was

performed by unpaired t-test on three independent biological samples (n= 40); ***p-value<0.001; error bars: SEM. B: Fluorescent image of *Tg(7xStat3:EGFP)* intestine at 6 dpf after 3 days of either 60µM AG-490 or DMSO treatment. Scale bar: 100µm. B': EGFP fluorescence quantification in the intestine of AG-490 and control larvae after 3 days of 60 µM AG-490 administration. Statistical analysis was performed by unpaired t-test (n=20); p<0.001; error bars: SEM. C: qRT-PCR analysis of *stat3*, *socs3a* and *EGFP* expression in EGFP-positive and EGFP-negative cells taken from adult intestines. Statistical analysis was performed by unpaired t-test (*p<0.05, **p<0.01, ****p<0.0001); error bars: SEM. D: immunofluorescence against mouse Stat3 (red spots) and colocalization with EGFP fluorescence of *Tg(7xStat3:EGFP)* larvae injected with CMV-m*Stat3C* plasmid. Scale bar: 10µm. E: Live image of the intestine of 7 dpf *stat3*$^{-/-}$*/Tg(7xStat3:EGFP)* and *stat3*$^{+/+}$*/Tg(7xStat3:EGFP)* siblings. Scale bar: 100µm. E': EGFP fluorescence quantification in the intestine of WT and *stat3*$^{-/-}$ *Tg(7xStat3:EGFP*) larvae at 7 dpf. Statistical analysis was performed by unpaired t-test (*p=0,0211) (n=12). E'': qRT-PCR analysis of *EGFP* expression in the 7-dpf *stat3*$^{-/-}$*/Tg(7xStat3:EGFP)* larvae with respect to the *stat3*$^{+/+}$*/Tg(7xStat3:EGFP)* sibling. Statistical analysis was performed by unpaired t-test on three biological samples (*p<0.05); error bars: SEM.

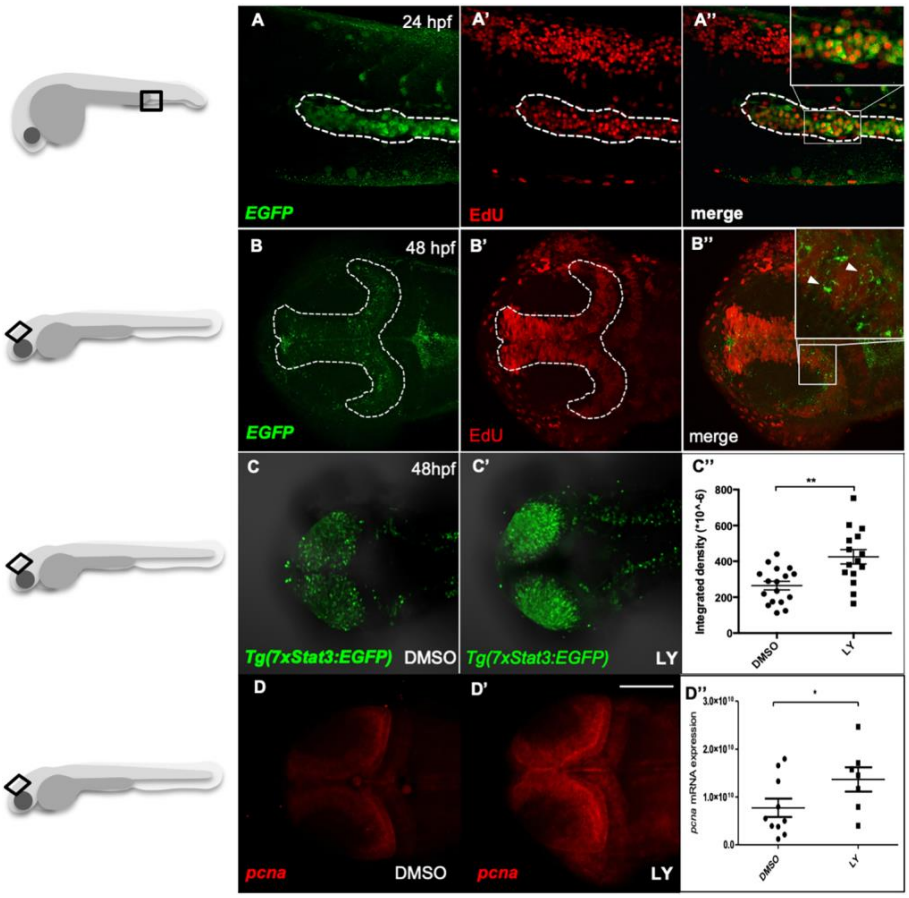

Fig. 3: Stat3 pathway is active in proliferating cells of zebrafish haematopoietic tissue and TeO. A-A'': Fluorescence co-localization (A") using α-EGFP Ab (A) and EdU proliferation assay (A') in the haematopoietic tissue (dashed line) of 22-hpf *Tg(7xStat3:EGFP)* reporter embryos. B-B'': Fluorescence co-localization (B") between FISH using α-EGFP probe (B) and EdU proliferation assay (B') in the optic tectum (dashed line) of 48 hpf embryos. C-C'': *in vivo* fluorescence of *Tg(7xStat3:EGFP)* reporter activity in the TeO of embryos treated with LY364947 inhibitor between 24-48 hpf (C') compared to DMSO-treated controls (C). Relative fluorescence intensity measured in the optic tectum of 48-hpf *Tg(7xStat3:EGFP)* embryos (n=15)(C''). Statistical analysis was performed by unpaired t-test. p=0.0014; error bars: SEM. D-D'': Whole mount *in situ* hybridization detection of *pcna* mRNA in the TeO of 48-hpf embryos treated with LY364947 inhibitor between 24-48 hpf (D') compared to DMSO-treated controls (D). Scale bar: 100 μM. Statistical analysis was performed by unpaired t-test. p=0.038; error bars: SEM.

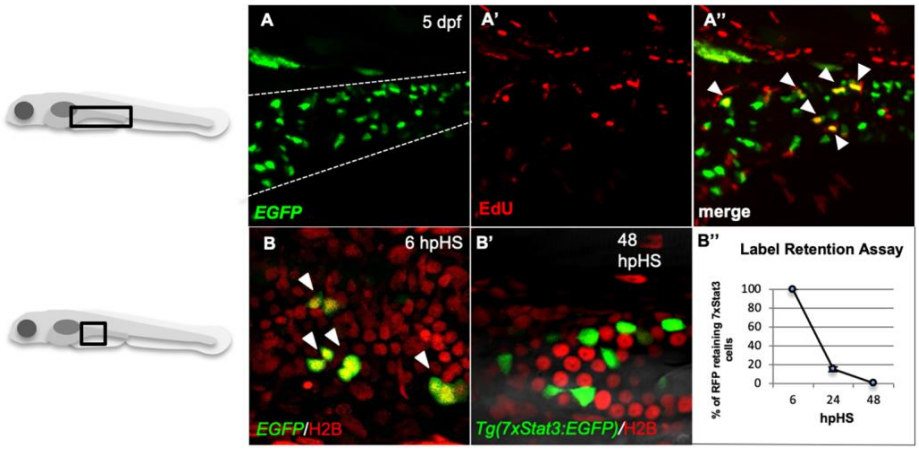

Fig. 4: Stat3 pathway is active in rapidly proliferating intestinal cells during zebrafish larval development. A-A'': Co-localization using α-EGFP Ab (A) and EdU proliferation assay (A') in the developing intestine (dashed line) of 5-dpf *Tg(7xStat3:EGFP)* larvae (A''). B-B'': Label retention assay using double transgenic *Tg(7xStat3:EGFP)/Tg(HSP70:H2B:mRFP)* 5 dpf larvae: ubiquitous RFP label, accumulated in 100% intestinal cells at 6 hours post heat shock (hpHS), is completely lost in EGFP expressing cells at 48 hpHS, where no EGFP/RFP co-localization is appreciable (B'). Graphical representation of RFP loss by *Tg(7xStat3:EGFP)*-positive intestinal cells. Three independent biological replicates were performed (B'').

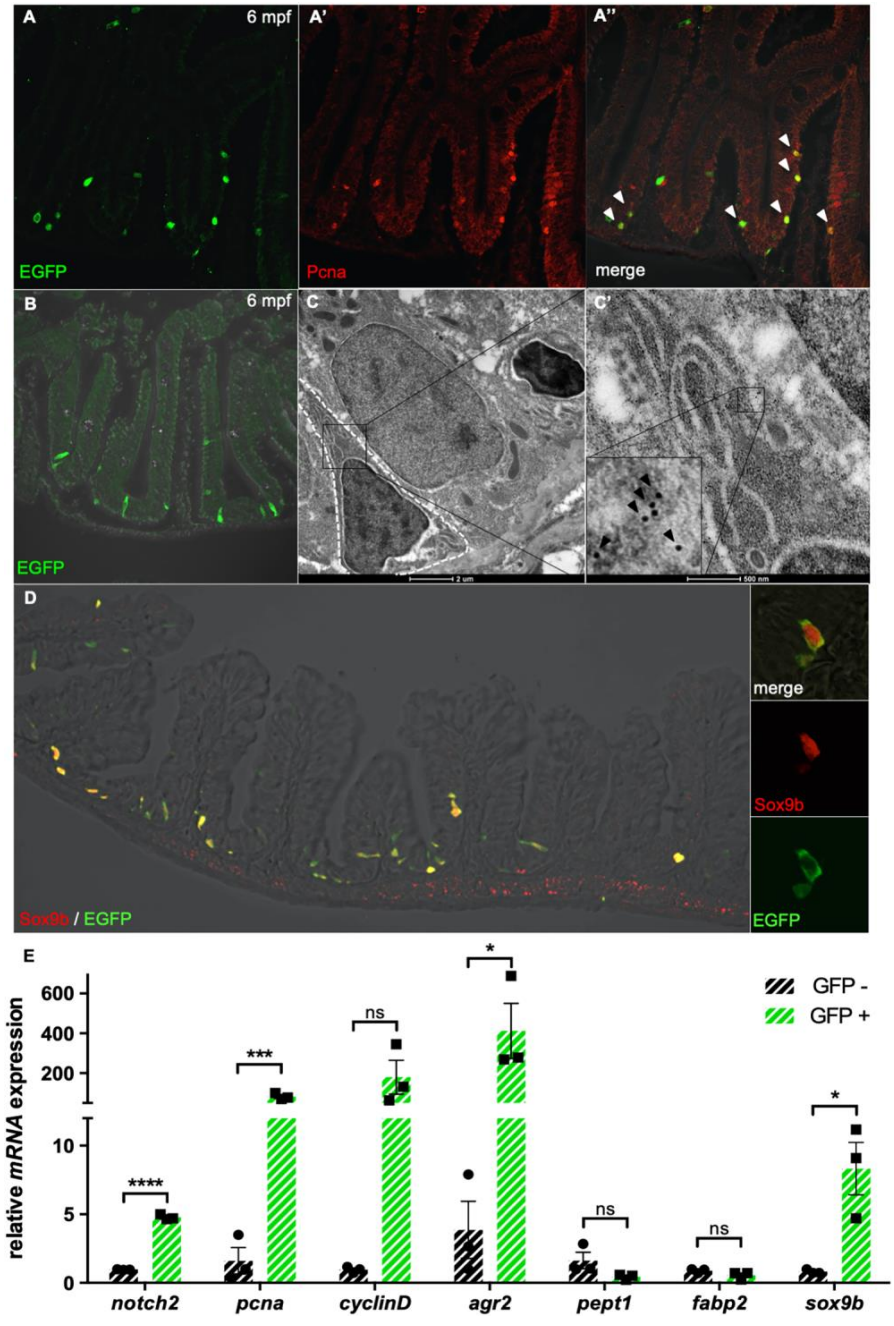

Fig. 5: Stat3 is active in intestinal FBC cells of adult zebrafish A: α-EGFP Ab (green)(A) and α-PCNA Ab (red)(A') staining of adult *Tg(7xStat3:EGFP)* intestine. B: staining with α-EGFP Ab on a transversal section of adult *Tg(7xStat3:EGFP)* intestine showing that all Stat3 positive cells are located at the base of the intervillus pocket. C-C': Immunogold staining with α-EGFP Ab on adult *Tg(7xStat3:EGFP)* intestinal sections observed by TEM:

a gold-labelled cell is surrounded with a white striped line (C); high magnification of gold-labelled cytoplasm belonging to triangular-shaped Fold Base Columnar (FBC) cell and zoom (C') on gold dots (black arrowheads). D: staining with α-EGFP Ab (green) and α-Sox9b Ab (red) of adult *Tg(7xStat3:EGFP)* intestine. E: qRT-PCR analysis of *notch2*, *pcna*, *cylcinD1*, *agr2*, *pept1*, *fabp2* and *sox9b* expression in EGFP-positive and EGFP-negative cells taken from adult intestines. Statistical analysis was performed by unpaired t-test (*p<0.05, ***p<0.001, ****p<0.0001, ns=not significant); error bars: SEM.

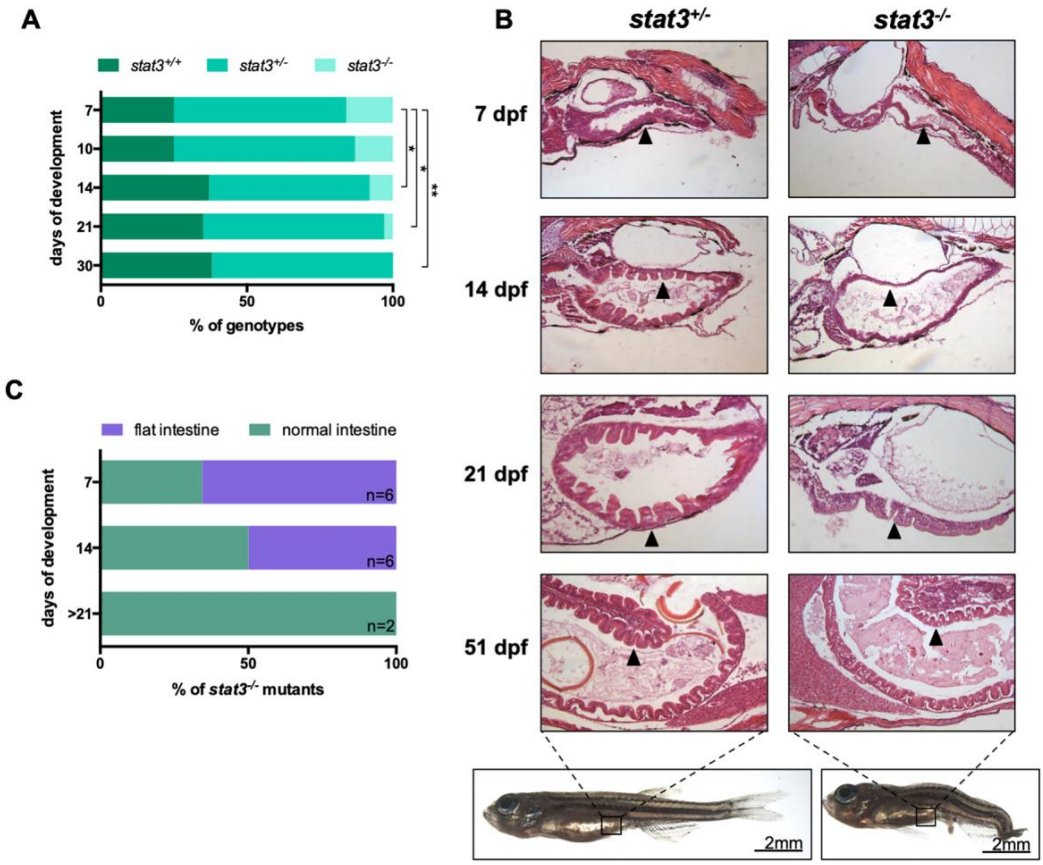

Fig. 6: Stat3 is required for intestinal homeostasis and larvae survival during development. A: Graphical representation of the percentage of the different genotypes found at different time points in *stat3*$^{+/-}$ incross; *stat3*$^{-/-}$ mutants were never found after 25 dpf, with the only exception of single animal that died at 51 dpf (showed on panel B). Statistical analysis was performed by chi-square test to compare proportions; *p-value<0.05; **p-value<0.01. B: Hematoxylin and eosin staining of longitudinal sections at different larval stages (indicated on the left); arrowhead indicates the intestinal epithelium; when compared to normal fish, mutants display flattening of the intestinal epithelium. C: Graphical representation at different stages of the percentage of individuals presenting either normal or degenerated intestine lacking intestinal folds.

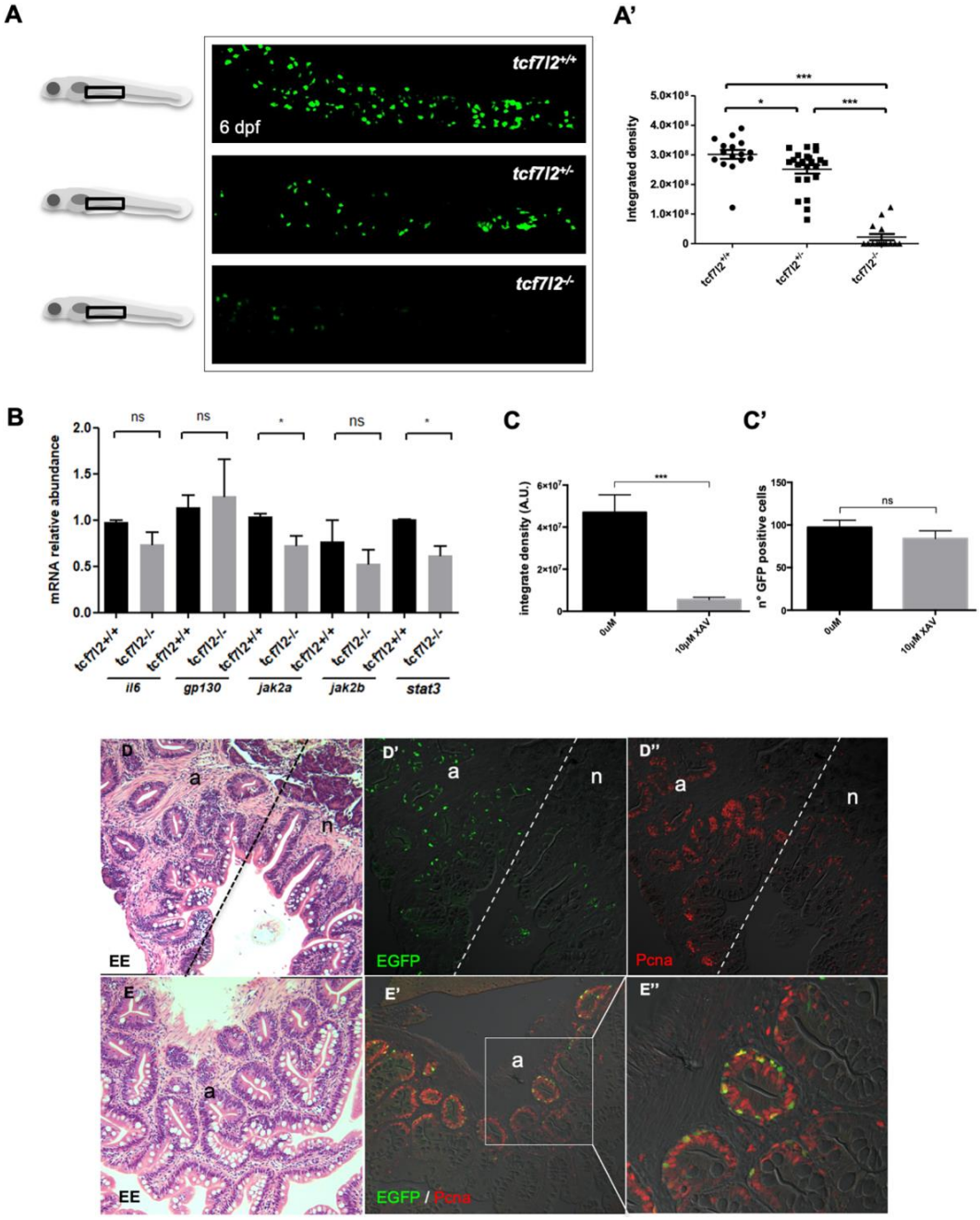

Fig. 7: Tcf7l2 (Tcf4) is required for development of Stat3 responsive cells of zebrafish larvae intestine and Stat3 pathway is activated ectopically in intestinal adenomas of *apc*^{hu745}- A-A': *In vivo* EGFP fluorescence in the intestine of 6-dpf *Tg(7xStat3:EGFP)/tcf7l2*$^{hu892/hu892}$, *Tg(7xStat3:EGFP)/tcf7l2*$^{+/hu892}$ and *Tg(7xStat3:EGFP)/tcf7l2*$^{+/+}$ siblings (A) and measurement of integrated density (A') (n=16). B: qPCR analysis of *il6*, *gp130*, *jak2a*, *jak2b* and *stat3* mRNA expression from *tcf7l2*$^{+/+}$ and *tcf7l2*$^{hu892/hu892}$ sibling larvae. Statistical analysis was performed by unpaired

t-test (*p<0.05); error bars: SEM. C-C': XAV treatment on *Tg(7xStat3:EGFP)* embryos from 48 hpf to 78 hpf, measurement of the integrated density of the fluorescence (C) and measurement of the number of GFP+ cells (C'). D, E: Hematoxylin and eosin staining on paraffin embedded transversal section of 12-month post fertilization (mpf) zebrafish *apc*^{hu745} intestine, displaying both normal tissue (n) and hyperplastic adenomas (a). D'-D'': staining of a sequential intestinal section of (D) by using α-EGFP Ab (green)(D') and α-PCNA Ab (red)(D''). E' and E'': Double staining using α-EGFP Ab (green) and α-PCNA Ab (red) of a sequential intestinal section of (E). Statistical analysis was performed by unpaired t-test. *p-value>0.05; **p-value<0.01; ***p-value<0.001; error bars: SEM.

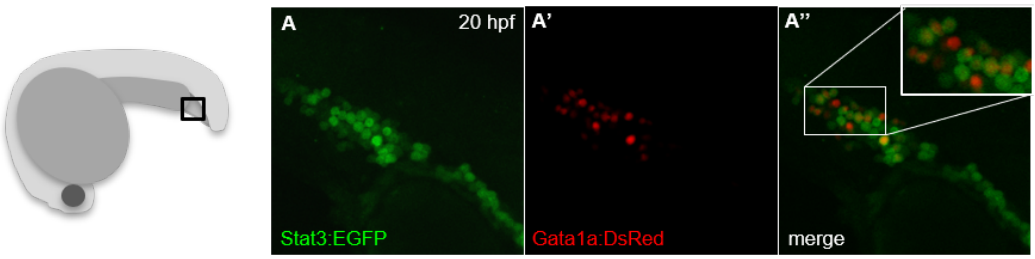

Fig. S1: Stat3 reporter is expressed in erythroid progenitor cells. A-A'': Confocal lateral view of haematopoietic tissue of double transgenic embryos obtained crossing the *Tg(7xStat3:EGFP)* (A) with *Tg(gata1a:DsRed)* (A'').

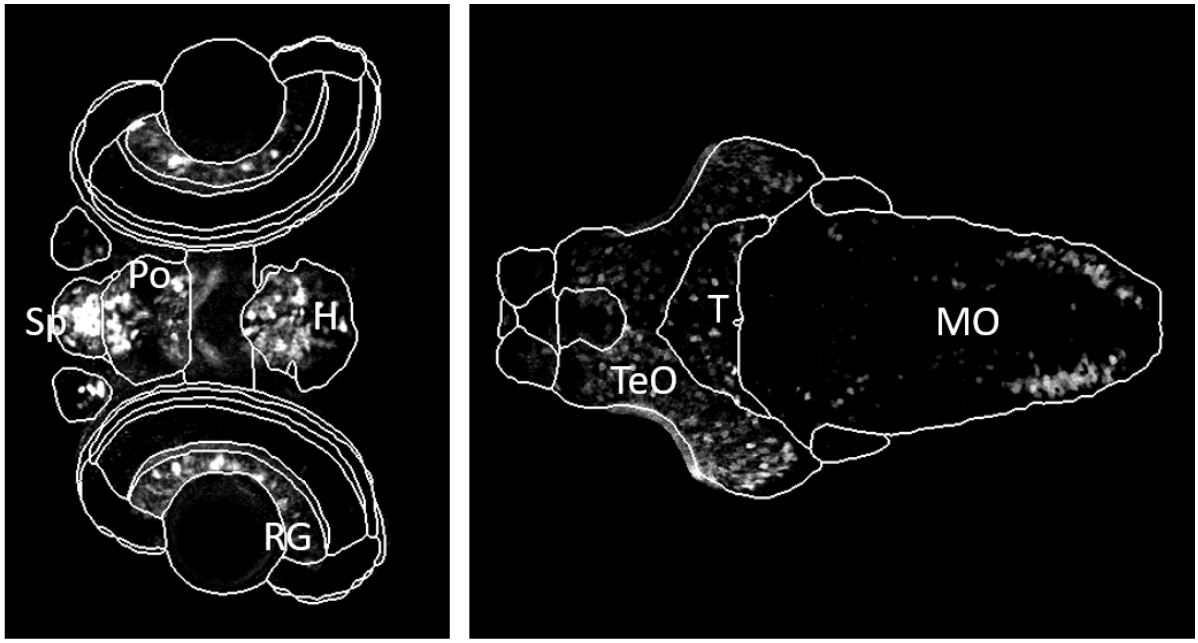

77 Tectum opticum (TeO)
97 Medulla oblongata (MO)
81 tegmentum (T)
7 subpallium (Sp)
45 preoptic region (Po)
48 hypothalamus (H)
59 retinal layer (RG)

Fig. S2: ***Tg(7xStat3:EGFP) reporter expression in the brain of 72-hpf larvae*****.** A-B: Single planes of *Tg(7xStat3:EGFP)* brain at 72 hpf. Images have been obtained with VIBEZ-Z software. H= hypothalamus, Sp= subpallium, Po= preoptic region, RG= retinal layer, TeO= tectum opticum, MO=medulla oblongata, T= tegumentum.

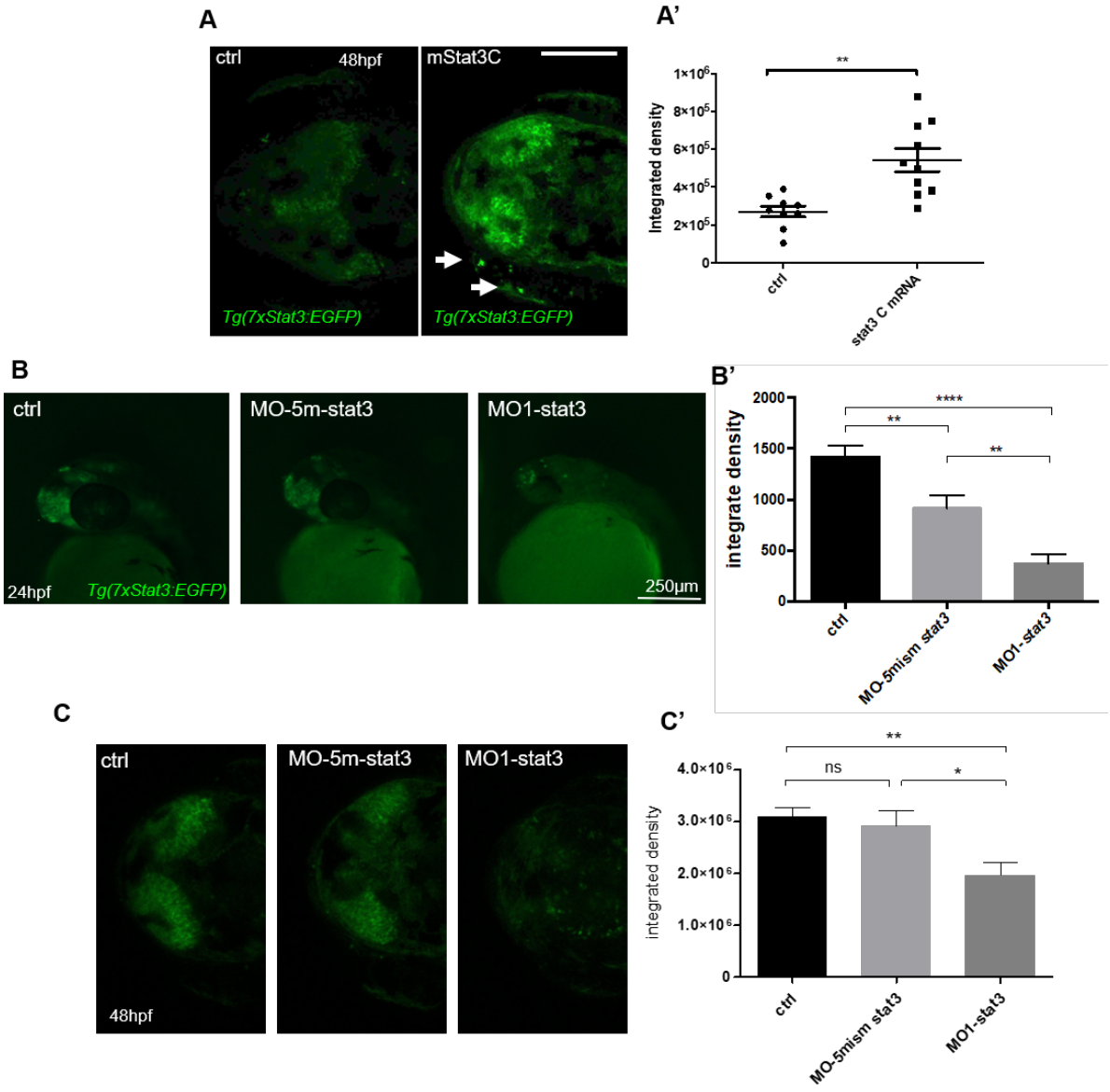

Fig. S3: *Tg(7xStat3:EGFP)* reporter line respond to silencing and overexpression of *stat3*. A: Dorsal view live image of the head of *Tg(7xStat3:EGFP*) controls (left) or m*Stat3C* mRNA injected embryos (right) at 48hpf. Arrowheads highlight ectopic fluorescent signal. Scale bar: 100µm. A': EGFP fluorescence quantification in the TeO of m*Stat3C* injected and control larvae at 48 hpf. Statistical analysis was performed by unpaired t-test (n=20); **p<0.01 B: representative pictures of 24-hpf *Tg(7xStat3:EGFP)* injected with stat3-MO1 (Liu *et al.,* 2017; Miyagi *et al.,* 2004; Yamashita *et al.,* 2002) 5-mismatch morpholino B': Quantification of EGFP fluorescence in 24-hpf embryos injected with stat3-MO1 morpholino and 5-mismatch morpholino on the reporter line. Scale bar=250µm, statistical analysis was performed by unpaired t-test on 3 biological replicates. **p<0.01, ****p<0.0001; error bars=SEM. C: dorsal view of 48-hpf *Tg(7xStat3:EGFP)* injected with stat3-MO1

and 5-mismatch morpholino. C': Quantification of EGFP fluorescence in 48-hpf *Tg(7xStat3:EGFP)* embryos injected with stat3-MO1 morpholino and 5-mismatch morpholino. *p<0.05, **p<0.01; error bars=SEM

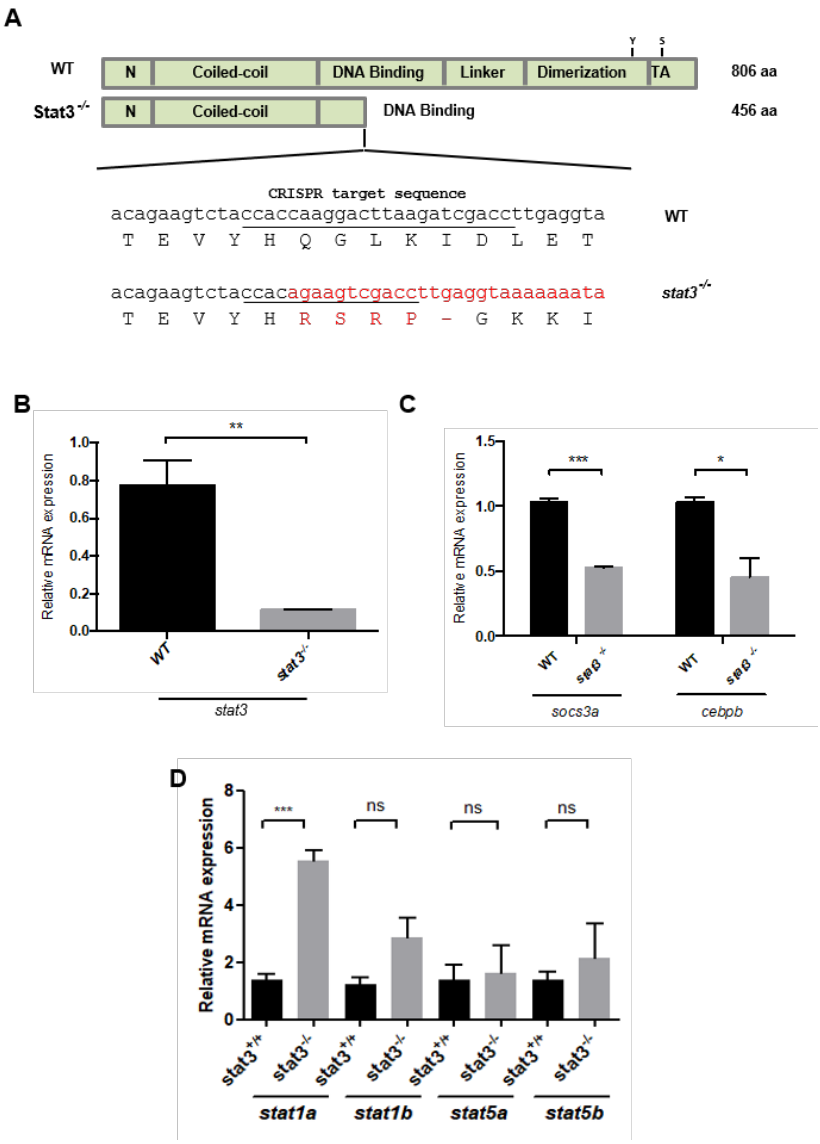

Fig. S4: *stat3*^{ia23} mutant validation. A: Schematic representation of *stat3*$^{-/-}$ mutant allele in comparison with WT. B: qRT-PCR analysis of *stat3* mRNA expression normalized on *gapdh* from WT and *stat3*$^{-/-}$ siblings at 6 dpf (p-value= 0,0073). C: qRT-PCR analysis of *socs3a* and *cebpb* Stat3 targets expression normalized on *gapdh* from WT and *stat3*$^{-/-}$ siblings at 6 dpf, *zgapdh* was used as internal control (p-values= 0,001; 0,0205); Statistical analysis was performed by unpaired t-test on 3 independent biological samples. **p<0,01; error bars=SEM. D: qRT-PCR analysis of *stat1a*, *stat1b*, *stat5a* and *stat5b* mRNA expression levels normalized on *gapdh* from *stat3*$^{+/+}$ and *stat3*$^{-/-}$ siblings at 6 dpf (***p<0.001)

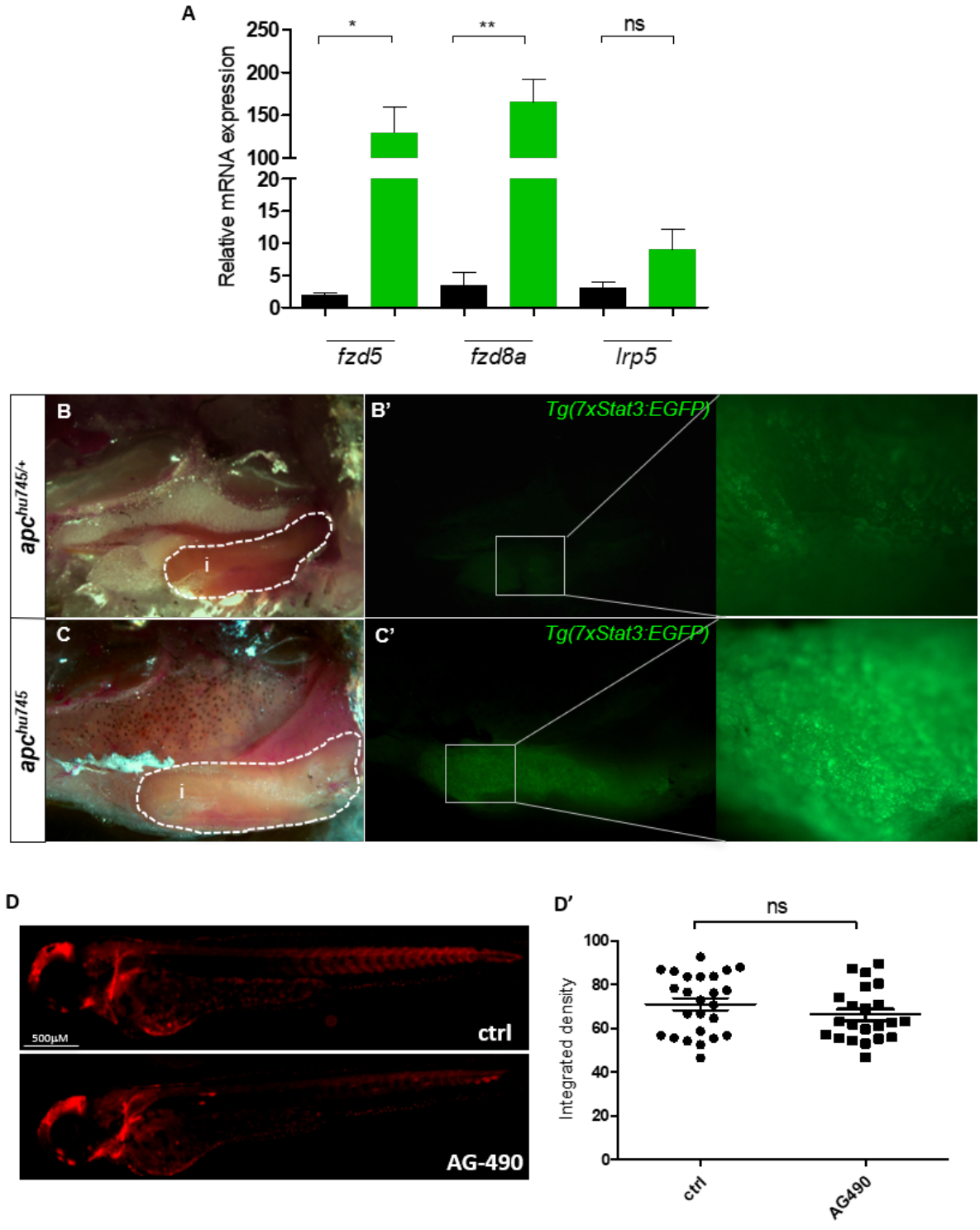

Fig. S5: Stat3 pathway is strongly activated in zebrafish *apc*-driven tumor. A: qRT-PCR analysis of *fzd5*, *fzd8a* and *lrp5* on EGFP-positive and EGFP-negative cells sorted from adult intestines. B-C'': *In vivo* EGFP expression is ectopic in 12 mpf *Tg(7xStat3:EGFP)/apc^{hu745}* hyperplastic intestine (B-B') with respect to *Tg(7xStat3:EGFP)/ apc$^{hu745/+}$* siblings (B-B'). C-C': representative pictures of 3-dpf

Tg(7xTCF-Xla.Siam:nlsmCherry)^{ia5} reporter larvae treated with DMSO and 80 µM AG-490 from 8-72 hpf (D); quantification of *Tg(7xTCF-Xla.Siam:nlsmCherry)*^{ia5} reporter larvae fluorescence (D'). Statistical analysis was performed by unpaired t-test. ns=not significant.

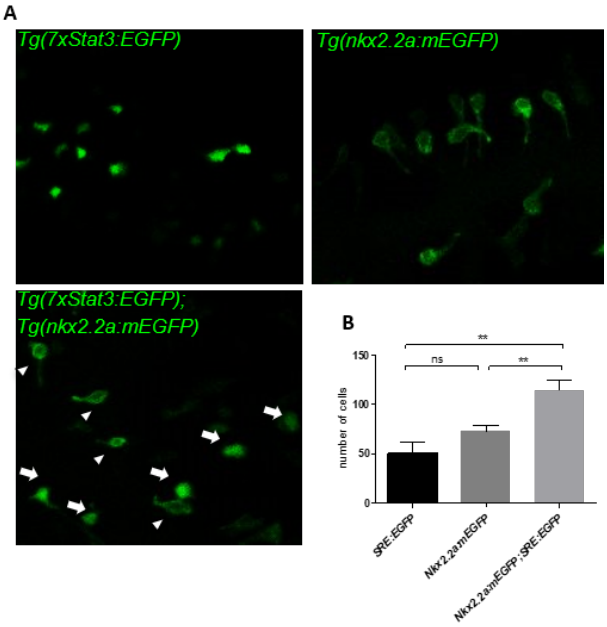

Fig. S6: EGFP positive cells of *Tg(7xStat3:EGFP)* zebrafish line are not secretory cells. A: representative prictures of *Tg(7xStat3:EGFP)*, *Tg(nkx2.2a:mEGFP)* and *Tg(7xStat3:EGFP)/Tg(nkx2.2a:mEGFP)* 6-dpf larvae intestine. B: number of EGFP-positive cells measured in intestines of *Tg(7xStat3:EGFP)*, *Tg(nkx2.2a:mEGFP)* and *Tg(7xStat3:EGFP)/Tg(nkx2.2a:mEGFP)* 6-dpf. Arrows indicate *Tg(nkx2.2a:mEGFP)* positive cells; arrowheads indicate *Tg(7xStat3:EGFP)* positive cells. **p<0.01, ns=not significant; error bars=SEM.

Gene	Forward primer sequence	Reverse primer sequence
zstat3	TGCCACCAACATCCTAGTGT	GCTTGTTTGCACTTTTGACTGA
zgapdh	GTGGAGTCTACTGGTGTCTTC	GTGCAGGAGGCATTGCTTACA
zcebpb	CCAAAAGTAACGGGCGACAC	ATCTTCCCTTACCTGACGGC
zsocs3	GGAAGACAAGAGCCGAGACT	GCGATACACACCAAACCCTG
egfp	ACGTAAACGGCCACAAGTTC	AAGTCGTGCTGCTTCATGTG
zstat1a	GCAGCTCAAGAAACTCCTGG	AAAGGTCTCTGCAGTTGGGT
zstat1b	CGAGTGGAAGAAGAGACAGC	GCTGGCCCCTTCCTAGATTT
zstat5a	TGACCCGAGAAGCTAACACC	GTATGTCCAGTCCTCCCT
zstat5b	TGAGGAAACAGCAAACCGTG	GCTGCTGAGTCAAGTGTTCA
zil6	CGTAAAGAGTCTCCTTGGCG	GGTTTGAGGAGAGGAGTGCT
zgp130	TGCTGGAGTGGGTGAATGAA	GGCTTGGTTACTGGTGTTCC
zjak2a	CTTCGAGAGTCAGGAGCCC	CTGAAGCTTCTTCACCGCC
zjak2b	ACGTATTGTGATTTCGCGGA	ACAAAAGACAAGGCCTGCAT
zsox9b	CTCGGCAAACTCTGGAGACT	GCGCATTGGTGGAGATCTG
zagr2	GCACAGACATACGAGGAAGC	GGAGACAAGTGCTTATCTGTG
zpept1	GATTGCTTTGGGAACAGGAGG	GATGGGTGTGATGAGAGTGG
zfabp2	GCTGCCCATGACAACCTG	CGTGTCTCCCTCTATGACC
znotch2	GACGAATGCATCTCCAGTGC	GCAGCAGCCACAGCAACC
zpcna	CCTTGGCACTGGTCTTTGAA	GGCACACGAGATCATGACAG
zcyclinD1	CCAACTTCCTCTCGCAAGTC	TGGTCTCTGTGGAGATGTGC
zfzd5	CCTAACTGTGCACTGCCTTG	ATTTGAAGCGCTCCATGTCG
zfzd8a	TGCAATCGGGAGTATGACGT	CTCGTTTCCCCACTTCATGC
zlrp5	TTCTCGGAGGGCCTGATTTT	TTGTCTCCGAGTCAGTCCAG

Tab. 1: list of primer used for Real Time qPCR.